Chloride Ingress and Corrosion of Steel Bars in Reinforced Concrete Made with Different Aggregates

by

Mahfuzur Rahman

MASTER OF SCIENCE IN CIVIL ENGINEERING

October, 2020

RECOMMENDATION OF THE BOARD OF EXAMINERS

The thesis titled "**Chloride Ingress and Corrosion of Steel bars in Reinforced Concrete Made with Different Aggregates**" submitted by Mahfuzur Rahman, Student ID: **171051017,** Academic Year 2018-2019 has been found as satisfactory and accepted as partial fulfillment of the requirement for the degree of Master of Science in Civil Engineering.

1. _____
Dr. Md. Tarek Uddin, PEng. — Chairman
Professor — (Supervisor)
Department of Civil and Environmental Engineering (CEE)
Islamic University of Technology (IUT),
Gazipur, Bangladesh.

2. _____
Prof. Dr. Md. Rezaul Karim. — Member
Head — (Ex-Officio)
Department of Civil and Environmental Engineering (CEE)
Islamic University of Technology (IUT),
Gazipur, Bangladesh.

3. _____
Dr. Moinul Hossain — Member
Professor
Department of Civil and Environmental Engineering (CEE)
Islamic University of Technology (IUT),
Gazipur, Bangladesh.

4. _____
Dr. A. F. M. Saiful Amin — Member
Professor — (External)
Department of Civil Engineering
Bangladesh University of Engineering and Technology.

Declaration

It is hereby declared that this thesis report or any part of it has not been submitted elsewhere for the award of any Degree or Diploma.

Name of Supervisor:
Dr. Md. Tarek Uddin, PEng.
Professor
Department of Civil and Environmental Engineering
Islamic University of Technology
Board Bazar, Gazipur 1704.
Date:

Name of Candidate:
Mahfuzur Rahman
Student No: 171051017
Academic Year: 2018-19
Date:

Dedication

I would like to dedicate this thesis to my parents and all my teachers who brought me up to this moment.

TABLE OF CONTENTS

LIST OF TABLES

LIST OF FIGURES

Acknowledgements

Glory and praise be to Allah the Almighty for giving me the strength and courage to successfully complete my M.Sc. thesis. Verily there is no strength except with Allah.

First of all, I would like to acknowledge the support and motivation of my thesis supervisor Prof. Dr. Md. Tarek Uddin, to whom, I owe my sincere appreciation for letting me be a part of his research project upon which this thesis is based. He has been a true inspiration that led me into research field of Concrete Technology. It is only through his concern, encouragement, and motivation that this work was completed. I am forever indebted.

A note of thanks is also extended to Prof. Dr. Md. Rezaul Karim, Dr. Moinul Hossain and Dr. A. F. M. Saiful Amin, who served on my Master's Thesis Committee, for their time and thoughtful review.

I wish to express my sincerest thanks and appreciation to laboratory technicians, and laboratory assistants of the Concrete Lab of Department of CEE, IUT for their constant help.

Finally, I am forever indebted to my parents, who raised me with love and supported me in all my pursuits, and for their understanding, endless patience, and encouragement. They form part of my vision that defined the good things that really matter in life.

I also acknowledge the financial support provided by the Bangladesh Road Research Laboratory (BRRL) and Islamic University of Technology to conduct this study. And also acknowledge the laboratory and other associated facilities provided by the Department of Civil and Environmental Engineering, Islamic University of Technology (IUT), Gazipur to carry out this study.

Abstract

Chloride-induced corrosion of reinforced concrete structures is one of the main reasons of deterioration of concrete structures in the marine exposures. A detailed investigation was carried out to compare macro-cell, micro-cell corrosion progress and chloride ingress in concrete made with different types of aggregates, such as recycled brick aggregate (RBA), fresh brick aggregate (BA) and stone aggregate (SA) as coarse aggregate. As fine aggregate natural river sand (NS) and recycled brick fine aggregate (RBFA) were used. CEM Type I (Ordinary Portland Cement (OPC)) was used as binding material. Cement contents were 340 and 400 kg/m^3. W/C ratios were 0.45 and 0.55. For investigation, reinforced specimens were made. As reinforcement both deformed bars and epoxy coated bars were used for investigation. Both cracked and un-cracked specimens were investigated. A total 16 cases was investigated. The cracked prism specimens were splashed with natural seawater one in a day. Un-cracked cylindrical specimens were submerged in 3% NaCl solution of temperature 40^{0}C for 180 days. The cylindrical specimens were cut to collect concrete samples from the depths of 0-10, 10-20, 20-30, 30-40 and 40-50 mm. Chloride profiles in concrete were evaluated by titration with $AgNO_3$ solution at 120 and 180 days of exposure. The recycled brick aggregate showed the highest level of chloride ingress compared to the other aggregates. The rate of macro-cell corrosion with respect to the type of aggregate is ordered as recycled brick aggregate (RBA) > fresh brick aggregate (BA) > stone aggregate (SA). It was also observed that chloride ingress as well as corrosion formation rate reduces with the increase of cement content and decrease of W/C ratio. No significant amount of corrosion was observed for the cases with epoxy coated bars.

CHAPTER 1: INTRODUCTION

1.1 General

Concrete is the most extensively used construction material around the world. Concrete is considered to be the 2nd most widely used material in the world after water. Concrete consumption in the world is estimated at three tons per capita per day (Gaag, 2014). To make this huge volume of concrete around 55 billion tons of aggregates are used worldwide every year. Concrete is one of the most frequently used building materials. Its usage worldwide is twice that of steel, wood, plastics, and aluminum combinedly (Cement trust, 2012).

Concrete has high alkalinity with pH level more than 13 that protects steel bars embeded into it by forming a passivation film around the steel bars naturally. Generally, after casting of concrete a thin passive flim of iron oxide of thickness having 10^{-3} to 10^{-1}μm forms surrounding the steel bars (Mohammed et al., 2001). But this passivation flim can be damaged due to certain level of chloride penetration in concrete which is known as chloride threshold limit. Chloride threshold limit is defined as 0.4% of cement mass or 1.2 kg/m^3 of concrete (Relim, 1988). Although reinforcement in concrete provides resistance against tension forces but due to corrosion in reinforcement the structure do fail consequently (Mohammed et al., 2003) and causes a wide range of economic losses around the world (ACI, 1996). From a structural point of view corrosion of steel may not immediately affect the ultimate load bearing capacity of reinforced structural member, it is the most insidious and destructive form of damage such that once it starts it is very difficult to stop the process and eventually the safety, stability and design life of the structure get drastically reduced with the passage of time. The immediate effect of steel corrosion is scaling, spalling and splitting of the cover concrete due to expansion of the corrosion products which can lead to loss of serviceability and integrity of structure. In marine structures the economic effect of structural damage can outweigh all considerations of

initial design costs and subsequent maintenance costs so that corrosion protection in reinforced concrete structures have become an essential factor of the design philosophy. Chloride ion penetration can arise from variety of sources such as from concrete mix constituents, from marine environment, from de-icing salts directly or indirectly through surface water or traffic spray. Chloride induced corrosion of steel has been found to be the major from of steel corrosion affecting the service life of many concrete structures, particularly since it can proceed rapidly even in the absence of carbonation.

Generally, for producing concrete in Bangladesh brick aggregate and stone aggregate are used as coarse aggregate. Also, considering sustainability of construction materials, studies have been made on implementation of recycled brick aggregates for making new structures (Mohammed et al., 2013). Many studies have already been conducted regarding corrosion mechanisms and chloride ingress in concrete. But no detailed study have been made on chloride ingress and corrosion of steel bars embedded inside concrete considering different types of aggregates available in our country. With this background the study has been planned to evaluate chloride ingress and corrosion of steel bars in reinforced concrete made with different aggregates. This study will be helpful for making long term design of infrastructures at or near marine exposure.

1.2 Background

Bangladesh is a South Asian country with a population of 160 million living in 147,570 square kilometers (Sarker et al., 2015). Bangladesh due to its geographical location, is in the frontline of the battle against climate change. The country has faced over 200 natural disasters in the last 40 years with increasing frequency and intensity. Cyclone Sidr in 2007 was amongst the most devastating, affecting nine million people across 30 districts in southern Bangladesh. Among top 10 deadliest tropical cyclones in human history Bangladesh has faced 6 of them. Rapid urbanization of Bangladesh has created a booming construction industry. Bangladesh has ranked 6^{th} among the top 10 countries with highest risk of disasters. Bangladesh is prone to cyclones due to its social and geographical

conditions. Recently Bangladesh has been attacked with cyclone Amphan which was formed on Indian Ocean and started moving north over the Bay of Bengal. 55,667 houses were completely damaged, and around 162,000 partially damaged and 200 bridges and culverts, and 100km of roads were damaged (IFRC, 2020). Also coastal areas of Bangladesh had suffered from the serious damages caused by two devastating cyclones; Sidr in 2007 and Aila in 2009. The government and international cooperation agencies have been tackling with mitigating cyclone disasters, mainly through construction of cyclone shelters, which can accommodate 500-2,500 people per shelter in case of cyclones (Mari et al., 2017). Existing number of cyclone shelters in Bangladesh is around 2200 but unfortunately, by 2005 most of these infrastructures had become hazardous due to chloride induced corrosion. At present around 4100 cyclone shelters are under construction which is also being subjected to chloride induced corrosion. This problem leads to huge amount of economic losses every year in our country.

The reinforced structures at coastal areas are not designed as per durability based design. Rather they are designed only considering the structural loads. Lack of durability based design is the main reason of failure of reinforced structures at coastal areas. In the coastal areas chloride penetrates into concrete and attacks reinforcements. Chloride induced corrosion is the main reason behind the deterioration of most of the reinforced concrete structures in coastal regions. Already many studies have been done on chloride ingress for different types of cements, rebar coating patterns. But no study has been done yet regarding chloride ingress and corrosion of steel bars in reinforced concrete considering different types of aggregates.

The most commonly used coarse aggregate in Bangladesh is brick aggregate. The department of environment reported that 4,000 brick kilns burn nearly 2 million tons of coal and 2 million tons of wood every year to meet the demand of 400 to 1200 tons of fuel (Hossain, 2012). Therefore, brick industry is associated with a lot of negative environmental impacts, including air pollution and loss of fertile land. Another commonly

used coarse aggregate is stone chips. The problem with stone chips is that, it is very expensive and need to be imported from India due to low availability in our country. Mining, dredging, and extraction of sand and gravel alter plant and animal habitats and contribute to soil erosion and air and water pollution. Mining for sand and gravel near or in water bodies causes sedimentation and pollution in water and disrupts aquatic habitats. The operation of mining equipment consumes energy and releases emissions from internal combustion engines. Energy to produce coarse and fine aggregates from crushed rock is estimated by the Portland Cement Association (PCA)'s Life Cycle Inventory to be 35,440 kJ per tons. The energy to produce coarse and fine aggregate from uncrushed aggregate is 23,190 kJ per tons (Medgar et al., 2006). To reduce the environmental impacts, it may be the most important to minimize the amount of virgin materials use (Sakai, 2005). For sustainability of construction materials in Bangladesh, several studies have been conducted on possibility of recycling of demolished brick aggregate concrete in new construction works (Mohammed et al., 2015). Long-term durability of concrete made with recycled brick aggregate is also a concern to the engineers. With this background, a detailed study on chloride ingress and macro-cell, micro-cell corrosion of steel bars in concrete made with brick aggregate (BA), recycled brick aggregate (RBA), and stone aggregate (SA) has been planned.

1.3 Objective of the Study

The objectives of this study are as follows:

a. To evaluate chloride ingress in concrete made with different aggregates, such as brick aggregate, stone aggregate and recycled brick aggregate.

b. To evaluate macro-cell and micro-cell corrosion of steel bars in concrete made with different aggregates, such as brick aggregate, stone aggregate and recycled brick aggregate.

c. To evaluate the effectiveness of fusion bonded epoxy coated bar against chloride induced corrosion attack.

1.4 Research Methodology

A total 16 different cases was investigated for this study. For each case, four 100 mm x 200 mm sized cylindrical specimens and two 100 mm x 100 mm x 400 mm sized prism specimens were made. In total, 64 cylindrical specimens and 32 prism specimens were made. W/C ratios were 0.45 and 0.55. Sand to aggregate volume ratio was 0.44. Cement contents were 340 and 400 kg/m^3. In each prism specimen, two steel bars were placed, one as continuous bar to avoid collapse of the beams during cracking and one as segmented steel bar. The length of the continuous steel bar was 34 cm. The segmented steel bar were made by connecting three different segments with epoxy. The length of the end segments was 13.5 cm and the length of the middle segment was 5 cm. All the steel bars were pre-jointed with electric cables before casting concrete. The depth of the cover concrete was 20 mm. After 24 hours of curing in the molds, the specimens were de-molded and cured under wet jute bags for 28 days. To fix the location of crack at the middle of prism specimen, a notch (3 mm wide and 5 mm depth) was made at the center of the bottom face of the specimens. The specimens were cracked applying center point loading under a Universal Testing Machine (UTM). Then the specimens were anchored in pair by back-to-back support with a roller at the middle. After that the specimens were kept at a seawater spray chamber where natural seawater was sprayed on the specimens once in a day for five minutes. At each electrical junction, a 100 ohm resistance was used to measure voltage drop due to the flow of electrons. The voltage drops were recorded continuously by using a data logger. At the end of sea water exposure, Corro-Map device was used to determine micro-cell corrosion and concrete resistance amount. Half-cell potential values were measured using $Cu/CuSO_4$ half-cell. The cylindrical specimens were submerged in 3% NaCl solution of temperature 40^{o}C and were cut to collect concrete samples from the depths of 0-10, 10-20, 20-30, 30-40 and 40-50 mm. Chloride profiles in concrete were evaluated by titration with Silver Nitrate solution at 120 and 180 days of exposure. After completion of macro-cell corrosion current measurement, the prism specimens were broken open and steel bars located at both cracked and un-cracked regions of the specimens

were taken out for visual observation and measurement of corrosion area and the depth of corrosion pits.

1.5 Research Flow Diagram

For starting a research work the first and prime task is to select topic on which the entire research will be based on. For this research work, our topic was selected considering chloride ingress and corrosion formation on steel bars in aggregates for different types of aggregates generally used in Bangladesh along with recycled brick aggregate. A huge number of literatures were studied carefully on the similar topic. All the corrosion investigation and chloride ingress testing mechanisms were studied deeply from various research works. All the recent finding of similar literatures similar to our topic were studied elaborately. The limitations of the previous research works were evaluated and how some very new findings on our research topic can be added with the knowledge acquired from the previous research work were planned and our objectives of research work were determined accordingly. After setting the research objectives, all the cases and items of evaluations were set. As per planning different materials for preparing our samples were collected and crushed as per ASTM C33. Various physical properties of the aggregates such as unit weight, abrasion value, specific gravity, fineness modulus etc were evaluated. Then mix designs of all our cases were prepared and all the necessary reinforcement preparation such as cleaning rebar, drilling and connecting cables with the rebar etc were done for inserting them in the casting work. After casting work the prism specimens were placed in a spraying chamber and different measurement of macro-cell corrosion, micro-cell corrosion, half-cell potential, and chloride ingress amount were done using different devices. All the prism specimens were finally autopsied for making physical investigation of the inserted corroded rebars. After getting all the values the results and discussions were made. Various conclusions were drawn considering the obtained results. Finally future recommendations were proposed based on this research work. Outline of the research methodology is shown below on Fig. 1.1 using flow chart.

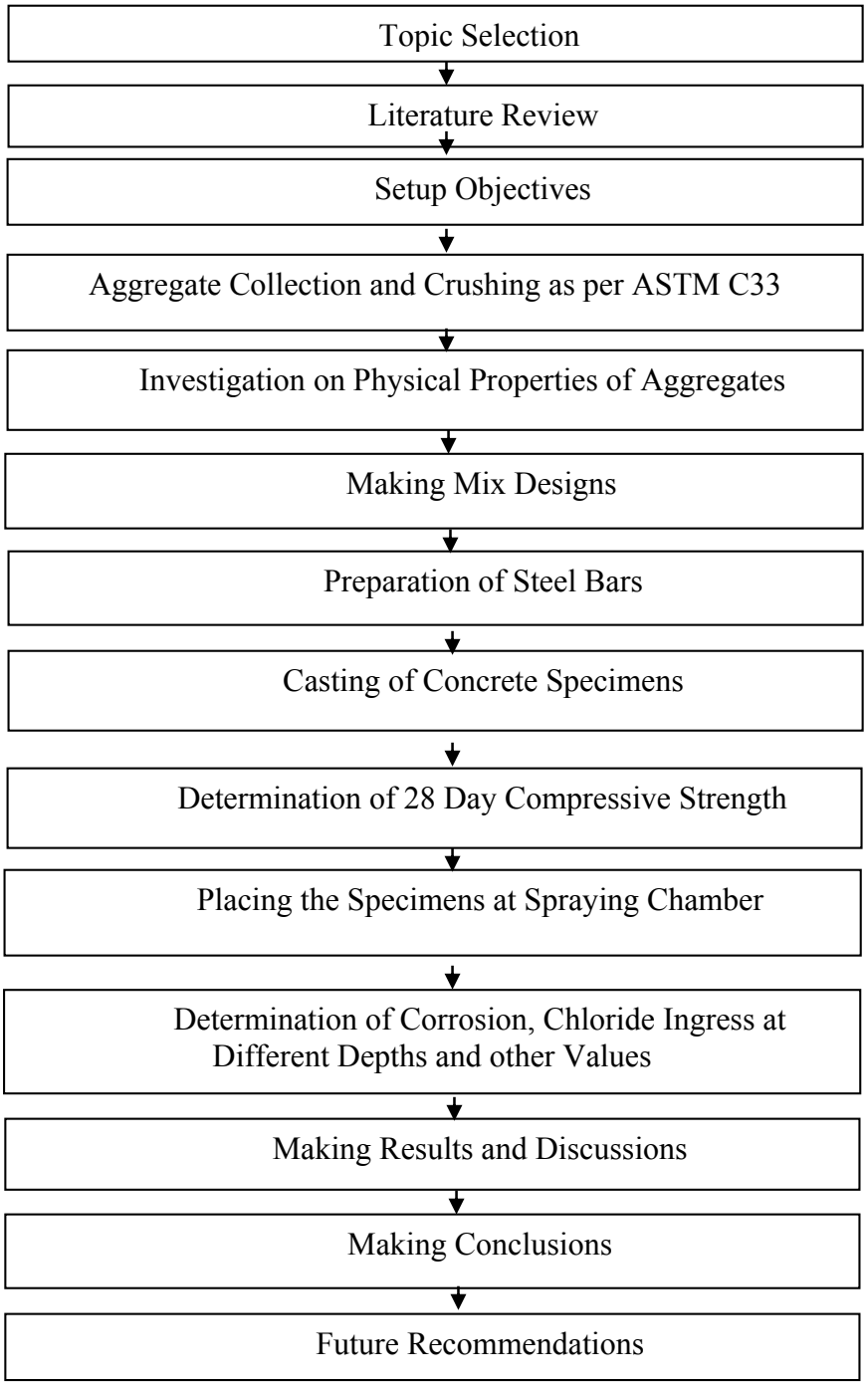

Fig. 1.1. Outline of Research Methodology

1.6 Layout of the Thesis

Chapter 1 thoroughly discusses the background and objectives of this study. Chapter 2 discusses about chloride penetration properties of concrete, factors of concrete affecting chloride penetrability, details of information of corrosion, corrosion characteristics, studies related to determine chloride ingress and corrosion formation in reinforced structures. Chapter 3 presents all the experimental methods, testing procedures, all the cases investigated, mix designs of this entire research work. The chapter concludes with information pertaining to the test methods and procedures followed in this study. Chapter 4 presents all the results obtained from this study. Results related to compressive strengths, chloride ingress amounts at different depths, macro-cell corrosion, micro-cell corrosion, concrete resistance, half-cell potential all are graphically represented in this chapter along with explanations. Chapter 5 presents a summary of the conclusions drawn from the results of this research and also suggests recommendations for future works.

CHAPTER 2: LITERATURE REVIEW

2.1 General

Reinforcement corrosion is one of the major deterioration mechanisms of reinforced concrete structures worldwide. The presence of chloride increases the rate of corrosion acutely. Therefore, this chapter discusses concrete in general as well as the corrosion mechanisms and chloride ingress variation for different types of aggregates commonly used in our country. This chapter also gives an overall review of the current state of research on corrosion of steel bars in concrete and chloride ingress process for different states of concrete.

2.2 Corrosion in Reinforcement

Corrosion of reinforcing bars inside concrete is one of the most important phenomenon's that reduce the service life of a concrete structure, and it causes a huge load on the maintenance budget of the affected structure. Concrete has poor tensile strength. To increase the tensile strength of concrete, steel reinforcement is used. Steel bars are embedded within the concrete mass. These steel bars carry most of the tensile load applied to the concrete. The concrete renders the steel bars passive due to its highly alkaline nature, thus preventing them from corrosion. Still, due to various reasons, the steel bars may get corroded. And due to the corrosion of the steel bars, various weaknesses arise in the concrete structure, which may eventually collapse if not taken proper care of within suitable time.

Corrosion of reinforcing steel embedded in concrete is an electrochemical process that requires an anode, a cathode, an electrolyte, and an electrical connection between the anode and cathode for transfer of electrons. Coupled anodic and cathodic reactions take place on the surface of the reinforcing steel. Concrete pore water acts as the electrolyte and the physique of reinforcement gives the electrical connection between the anode and

cathode. Cathodes and anodes may be placed on the same rebar (micro-cell) or on different bars (macro-cell) that are electrically related through metal ties or chairs. The process of steel corrosion inside concrete is defined as the removal of iron atoms (Fe) from steel and their dissolution in the surrounding water solution, appearing as ferrous ions (Fe^{+2}) (Bentur et al., 1997). Because of this dissolution, steel loses mass, and its section becomes smaller. Rust is a result of the corrosion process. For this process to occur, moisture and oxygen ought to be present, and both of them are available in concrete. However, due to the excessive alkalinity of interior concrete (pH > 13), steel will be in a position to form a very skinny flim called the passivation layer (Bentur et al., 1997), which acts as a protection coating that prevents the metal from taking section in the corrosion process. Unfortunately, this layer can be disrupted due to either carbonation or chloride ion attack. The chemical reactions are similar for each of them. Once initiated, corrosion products, which have higher volume than the parent metal, will accumulate in the space between the rebar and concrete, and since there is insufficient space to accommodate these products, cracking and spalling of the concrete cover will occur. If the rebar cross sectional loss is severe, structural problems may start to occur.

2.3 Corrosion Formation Principle

The first step in the rusting process involves the dissolution of solid iron into solution. The formula for this is:

$$Fe(s) \rightarrow Fe^{2+}(aq) + 2e^{-} \quad (2.1)$$

The electrons produced by this reaction combine with hydrogen ions in the water as well as with dissolved oxygen to produce water:

$$4e^{-} + 4H^{+}(aq) + O_2(aq) \rightarrow 2H_2O(l) \quad (2.2)$$

These two reactions produce water and Iron (II) ions, but not rust. For that to form, another reaction has to occur.

The consumption of hydrogen ions that occurs as iron dissolves leaves hydroxide) ions in the water. The Iron (II) ions react with them to form green rust:

$$Fe^{2+}(aq)+2OH^{-}(aq)\rightarrow Fe(OH)_2(s) \quad (2.3)$$

The iron (II) ions also combine with hydrogen and oxygen in the water to produce Iron (III) ions:

$$4Fe^{2+}(aq) + 4H^{+}(aq) + O_2(aq) \rightarrow 4Fe^{3+}(aq) + 2H_2O(l) \quad (2.4)$$

These iron ions are responsible for the formation of the reddish deposit that gradually eats holes in auto bodies and metal roofing worldwide. They combine with the extra hydroxide ions to form Iron (III) hydroxide:

$$Fe^{3+}(aq) + 3OH^{-}(aq) \rightarrow Fe(OH)_3 \quad (2.5)$$

This compound dehydrates to become $Fe_2O_3.H_2O$, which is the chemical formula for rust. The hydrated ferric oxide has a volume of three to six times that of the original volume of steel (Broomfield, 1997) and since there is not enough space at the steel concrete interface, these products will accumulate and cause tension stresses on the concrete cover. Eventually, these stresses will exceed the concrete tensile strength causing cracking and spalling of the concrete cover.

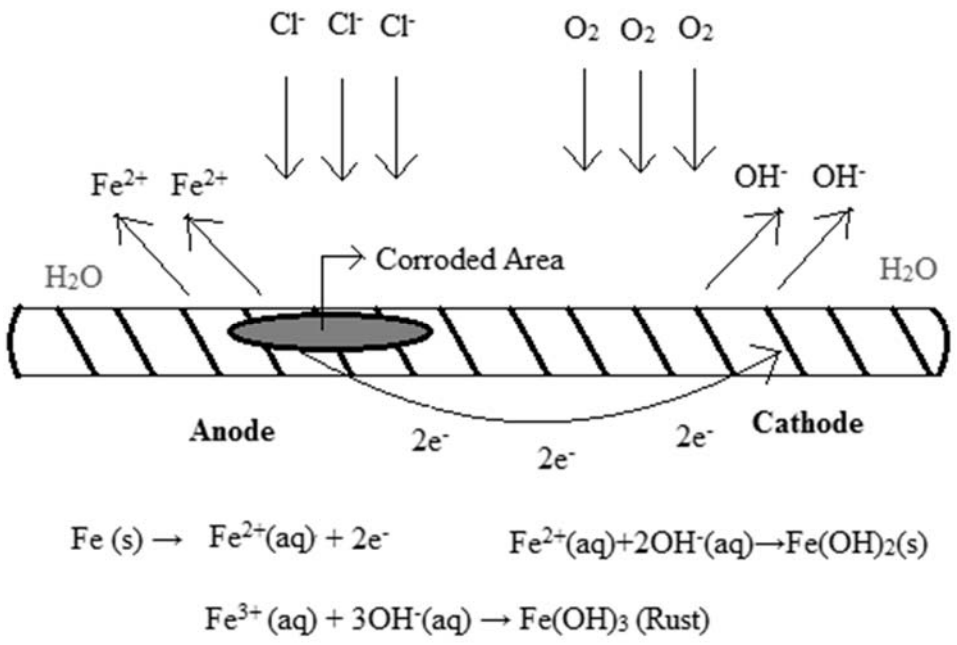

Fig. 2.1. Schematic Diagram for the Process of Steel Corrosion in Concrete

2.4 Carbonation Induced Corrosion

In the case of carbonation, atmospheric carbon dioxide (CO_2) diffuses through concrete and reacts with pore water alkalis according to the following reactions;

$$CO_2 + H_2O \rightarrow H_2CO_3 \quad (2.6)$$

$$Ca(OH)_2 + H_2CO_3 \rightarrow CaCO_3 + 2H_2O \quad (2.7)$$

Due to this reaction, the pH level of concrete gets reduced to 8-9 and the passivation flim around the steel gets broken and corrosion process begins. In other words, carbonation causes deterioration of the passive layer by reducing the concentration of the OH^- ions in

the concrete pore water. Thin concrete cover and poor concrete quality increases the risk of carbonation (Gaal, 2004).

Measuring the carbonation depth is done by exposing a fresh concrete surface to an indicator solution made with Phenolphthalein. The solution is colorless, will remain colorless on carbonated areas, and will turn pink on the alkaline sites. A fresh concrete surface can be obtained by cutting or splitting core concrete samples in the laboratory (Broomfield, 1997).

2.5 Chloride Ingress and Chloride Induced Corrosion

Chloride-induced corrosion is one of the most serious causes of concrete deterioration (Kropp, 1995). The penetration of chloride ion which generally comes from salt containing chlorine go through pores into permeable concrete is called chloride ingress. The strong nature of $Ca(OH)_2$ with pH > 13 prevents the corrosion of steel reinforcement by the formation of a thin protective film of iron oxide on the metal surface. When concrete is permeable, chloride from surrounding environment get penetrated to the reinforcement and the pH level of concrete adherent to reinforcement reduces to 11 or less than that. As a result the passivation flim gets destroyed and corrosion formation starts taking place.

Chloride penetration is done by two process, diffusion and absorption. When water and air is present, only then chloride starts corrosion process. For this reason no corrosion is observed due to chloride ingress in the dry concrete. Chloride ingress are due to permeability of hardened concrete and for selecting high water to cement ratio for wet concrete. With higher amount of permeability concrete is subjected to higher amount of corrosion. The source of chloride ions could be either external by using de-icing salts or from seawater in marine environments or internal by using contaminated aggregate or using concrete admixtures that contain chloride. This sort of depassivation is local and is

followed via a kind of corrosion referred to as pitting corrosion. On the contrary, the depassivation by means of carbonation will cause uniform corrosion on the entire rebar surface. The minimum amount of chloride ions required to initiate rebar corrosion is referred to as the chloride threshold limit. Chloride threshold limit may be expressed both as a percent of general or free chloride content per cement weight or as a ratio among the concentrations of chloride ion and hydroxyl ion dissolved inside the concrete pore water.

Some content of chloride in concrete may be physically or chemically bonded to the concrete matrix. Physical bonding occurs by chloride absorption on the surface of silicate hydrate or inside C-S-H gel (Arya and Newman, 1990). The chemical bond is due to the reaction of the tri-calcium aluminates C_3A with chloride ions to form $3CaO.Al_2O_3.CaCl_2.10H_2O$ which is known as fried salt (N & Song, 2007).

Both the total chloride content and the free chloride content of concrete can be measured by laboratory testing. First, core samples are taken from different depths. To measure the free components of chloride (water-soluble chloride), concrete dust can be boiled in water and then the concentration of chloride can be measured using chloride-sensitive electrodes. This process is described in ASTM standard C1218. To determine the total components of chloride (acid soluble chloride) titration should be applied to solid dust. This process is described in ASTM standard C1152. The total chloride content or free chloride content is then expressed as a percentage of the weight of the cement.

Researchers disagree on the role of bound chloride for corrosion of reinforcement inside concrete. Some have argued that bound chloride ions are immobilized and do not reach the surface of the rebar, so bound chlorides should not be considered when calculating the chloride limit (Hope et al., 1985 and Castelot et al., 2000). It has been suggested that the use of the Cl^-/OH^- ratio is more beneficial because it represents the competitive action of both ions and does not depend on the type of cement (Castelot et al., 2000). The most common method used to determine the Cl^-/OH^- ratio is the titration of the extracted concrete pore solution. Concrete pore solution can be squeezed out of concrete

or mortar samples by applying high pressure (up to 375MPa) on samples confined in a cylindrical pressure vessel (Barneyback and Diamond, 1981 and Page and Vennesland, 1983). However, this method of measuring Cl^-/OH^- has been criticized as expensive and difficult to manage. Recently, new methods based on chemical leaching have been used to extract free chlorides contained in the liquid phase. A large number of studies have been devoted to the study of the destruction of passive film by chloride ions, and three general models have been proposed: 1) adsorption-displacement, 2) chemical-mechanical and 3) migration-penetration. The strengths and weaknesses of each model is discussed in detail by Jovancicevic et al. (1986).

Chloride ions may be mixed into the concrete with contaminated ingredients and chemical admixtures or they may come from external sources such as deicing salt application, sea salt spray, and direct seawater spraying. Marine structures, especially sub structures, are exposed to severe corrosion due to the abundance of chlorides (Sagar 1994). Concrete bridges and parking garages have also deteriorated dangerously since the 1960s due to the use of de-icing salts which causes chloride-induced corrosion (Brick et al. 1988). Chlorides typically enter the concrete bridge deck or slab of parking garages from the top, reach the top reinforcement layer and initiate localized corrosion. Magnesium chloride, calcium chloride, and calcium magnesium acetate are among the deicing chemicals that are available on the market. One study found that magnesium chloride was the most destructive chemical, followed by calcium chloride (Cody et al., 1996).

As per the long term investigation made by (Sofia and Jose, 2018), they found permeability and w/c ratio as important factors for chloride ingress through concrete. Concrete with higher porosity subjected to higher amount of chloride ingress rate. On the contrary chloride ingress rate gets reduced with the reduction of w/c ratio.

Cement types have great impact on chloride ingress rate through concrete which have been investigated by Mohammed et al. (2019). As per the investigation it was found that slag cement had the highest resistivity against chloride ingress. The chloride ingress

in concrete with respect to the types of cement is ordered as CEM Type-II S-L> OPC> CEM Type-II B-L > Slag Cement as per the investigation.

Correlation between the chloride diffusivity and the imposed loading damage was established in a study conducted by Ma et al. (2019). In this study it was found that recycled aggregate concrete has higher amount of chloride penetration tendency than normal concrete. On the contrary it was found that recycled powder concrete has higher resistivity against chloride ingress due to having higher fineness.

Porosity as the most influencing factor for chloride ingress was concluded by Price et al. (2003). For different types of aggregates with different types of water absorption rate and porosity, it was found from the investigation that aggregates with higher porosity lead to higher amount of chloride ingress.

2.6 Macro-Cell and Micro-Cell Corrosion

Corrosion of steel reinforcement bars is basically an electrochemical reaction. Small anodes and cathodes are created and a flow of ions between these two electrodes lead to the corrosion of the steel bars. The total corrosion progress is divided into macro-cell and micro-cell corrosion. The magnitude of macro-cell corrosion is dominant at the early age, whereas the micro-cell corrosion is dominant in the later stage.

Macro-cell corrosion can occur when the actively corroding bar is coupled to another bar which is passive, either because of its different composition or because of different environment. Macro-cell corrosion is also known as Galvanic corrosion. Again, micro-cell corrosion is the term given to the situation where active corrosion and the corresponding cathodic half-cell reaction take place at adjacent parts of the same metal.

2.7 Prediction of the Service Life of RC Structure

The total service life of a reinforced concrete member subjected to corrosion of reinforcement is considered to be the sum of two phases: the initiation phase and the propagation phase shown in Fig. 2.2. This model was first introduced by Tuutti (1982). The initiation phase is the time required by chloride ions to penetrate the concrete cover and accumulate on the rebar surface until the critical limit is reached, or the time needed for the carbonation front to reach the rebar level, after this time, corrosion of the embedded rebar will start. The time elapsed in this phase is dependent on the chloride threshold level of the reinforcement material and its ability to remain passive when the pH of the surrounding environment drops due to carbonation. In addition, the initiation phase is dependent on the rate of transportation of the aggressive elements through the concrete cover. The propagation phase is the time dependent by corroding rebars to cause cracking and spalling of the concrete cover. Thus, the propagation phase is dependent on the corrosion rate of the metal, and the thickness and properties of the concrete cover.

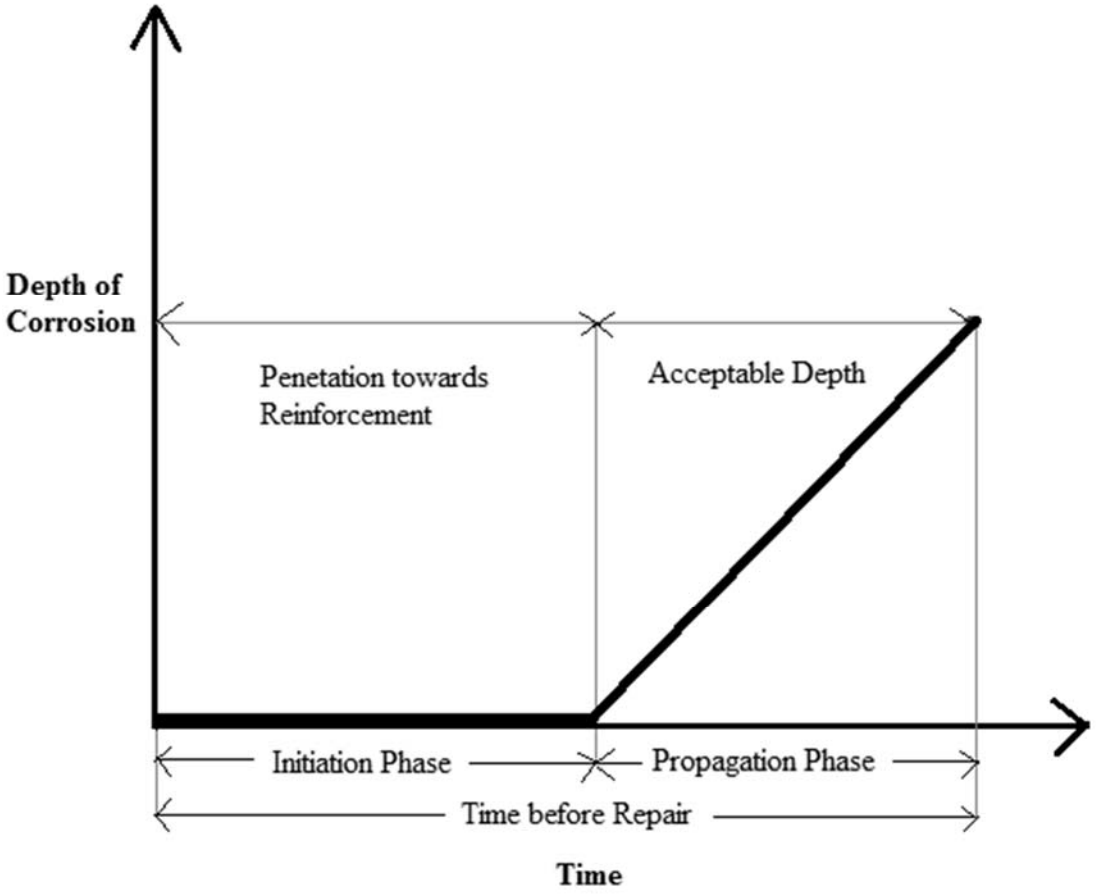

Fig. 2.2. Phases of Corrosion

2.8 Corrosion Monitoring Methods

Corrosion of steel bars is a serious problem for reinforced concrete structures and it can have a large economic impact. Several corrosion monitoring methods have been developed to mitigate the impacts of corrosion. A detailed review and analysis of available monitoring techniques was performed by Rodriguez et al. (1994). He reviewed and evaluated the monitoring techniques for speed of individual measurements, speed of response to change, provided quantitative information, destructivity, disturbing of sample and measurement parameters. Recently, more reviews of corrosion monitoring methods

have been evaluated including Surface potential (SP) measurements, Tafel extrapolation, galvanostatic pulse transient method, embeddable corrosion monitoring sensor, ultrasonic pulse velocity, X-ray radiography measurement, and infrared thermograph electrochemical methods (Song and Saraswathy, 2007). Change of resistance of reinforcement, an additional corrosion monitoring technique was proposed by Cella and Taylor (2000). They stated that this technique was more accurate than other more expensive electrochemical methods like the linear polarization resistance measurements. Different corrosion monitoring methods are shortly described below:

2.8.1 Half-Cell Potential

Half-cell potential is a commonly used corrosion monitoring method because of its simplicity. It is described in American National Standards ASTM C 876. A half-cell is used to determine the potential difference. The potential difference against a reference electrode at different points on a structure is measured as half-cell potential which determines the possibility of corrosion in reinforced structures. It does not give information regarding rate of change of corrosion. So, this method is used with other monitoring methods to determine the rate corrosion in a structure. Potential readings obtained by this method are interpreted following ASTM C 876. Standard Test Method for Half-cell Potentials of uncoated steel in reinforced concrete structures is shown on Table 2.1.

Table 2.1. Corrosion Interpretations (ASTM C 876)

Half-Cell Potential Reading (V)		Corrosion Activity
CSE	SCE	
>-0.200	>-0.125	Greater than 90% probability of no corrosion
-0.200 to -0.350	-0.125 to -0.275	An increasing probability of corrosion
<-0.350	<-0.275	Greater than 90% probability of corrosion

Here, CSE and SCE means Copper-copper sulfate electrode, saturated calomel electrode accordingly.

Many factors and properties of half-cell can affect the half-cell potential reading. Polarization can occur due to limited oxygen diffusion which can influence the potential significantly. When the oxygen diffusion is limited, especially when samples are immersed fully into a solution, potential value can fall to very negative values without any actual corrosion (Arup 1983; Elsener and Bohni 1992). High resistance layers in concrete can also affect the potential values. Many other factors such as conductivity of formed corrosion products, reference electrode position, cement type, the age of concrete and presence of cracks were reported as factors affecting the half-cell potential (Alonso et al., 1998; Browne et al., 1983; Elsener et al., 2003).

2.8.2 Macro-Cell Corrosion Rate

Structures that are exposed to chloride ions and high moisture condition such as: bridge decks, parking structures etc. are more prone to be corroded due to chloride ingress. High moisture contents reduce the resistivity of concrete and separate anodes and cathodes. The top reinforcement of mat becomes anode and the bottom reinforcement acts as cathode and thus macro-cell corrosion is formed in the structures (Wipf et al. 2006). The current flow is caused by the potential difference between the anode and cathode and corrosion takes place due to the current flow. The samples were made with two layers of reinforcement that were electrically connected through a resistor to observe the corrosion mechanism. Current flows between the reinforcement layers of reinforcement in the sample which can be determined by measuring the voltage drop over the resistor. Using Faraday's Law, corrosion rate can be calculated from the obtained voltage drop values. To measure macro-cell corrosion current for monitoring corrosion activity, ASTM G 109 method, southern exposure (SE) method, cracked beam method etc. are some of the well-known and widely used laboratory tests.

2.8.3 Polarization Resistance

Polarization resistance is another widely used corrosion monitoring technique. It is a non-destructive electrochemical method that determines the instantaneous corrosion current density, i_{corr}, of steel reinforcement using the assumptions in electrode kinetics. In this method, the potential of reinforcement relative to its open circuit potential is increased or decreased by a fixed amount E. The current decay, I due to the change in potential is monitored. A voltage-current density curve can be developed based on the result. The curve is linear in the vicinity of the open circuit potential (10 to 30 mV). The slope of the curve (Rp) of this section is defined as the polarization resistance, Rp (Stern and Geary 1957).

$$Rp = \frac{\Delta E}{\Delta i} \qquad \Delta E \to 0 \tag{2.8}$$

The potential can be changed potentiostatically where potential is changed in a fixed amount and current change due to the change in potential is measured. The potential can also be changed galvanostatically, where a fixed amount of current is supplied and the change in potential is monitored. Current density, I, is measured which is divided by the exposed surface area of steel bars. To calculate the instantaneous corrosion current density, i_{corr}, the Stern-Geary constant, B is divided by the slope value, Rp, shown in Eq. (2.8).

$$I_{corr} = \frac{B}{R_p} \tag{2.9}$$

The slope value Rp is in Ωcm^2 and B is in Volts. The Stern-Geary constant can be derived from anodic and cathodic Tafel coefficients, βa and βc. It is shown in Eq. (2.10):

$$B = \frac{\beta_a \beta_c}{2.3(\beta_a + \beta_c)} \tag{2.10}$$

A wide range of systems can affect the Stern-Geary constant value from 13 to 52 mV (Stern 1958). For reinforcing steel, the use of 26 mV for bare steel in the active state and galvanized steel and 52 mV for bare steel in the passive state was recommended by a study (Andrade and Gonzales 1978). Many studies also used 26 mV as B value. A recent study has shown that measuring B value from the measured E_{corr} values can provide better estimates and better correlations with weight loss measurements (Baweja et al. 2003).

A recent study by Chang et al. (2007) has shown that, performing the potential sweeps in the anodic and cathodic regions in two separate tests results in better potential current curves and also discussed that the surface of the reinforcing steel will not be affected by a sweep of ±120 mV. Videm (2001) and Andrade et al. (1995) also discussed that, the measured polarization resistance values may be affected by the amount of corrosion products build-up by consuming current in addition to that directly linked to corrosive reactions.

Due to the size mismatch of the small counter electrode and the large working electrode, a significant issue with the application of polarization resistance to on-site structures can arise. Electrical signals are not uniformly distributed over the entire metallic system like the laboratory samples with similar sized counter and working electrodes. With the increase of distance from the counter electrode, electric signals tend to decrease. To solve this problem, two methods were developed. The first method measures the polarization resistance based on a transmission line (Feliu et al., 1988; Feliu et al., 1989). In the other method, a guard ring is used to confine the distribution of electrical signal to a given area of the structure located below the counter electrode (Feliu et al., 1990). Sehgal et al. (1992) conducted experiments using the guard ring technique on-site and developed some techniques to obtain better accuracy. He indicated that the accuracy could be improved by using a planar concrete surface, decreasing the contact resistance between the probe and concrete surface, making measurements after the steady-state potential was reached and symmetric positioning of the probe over the reinforcement. Another more recent study evaluated the linear polarization resistance technique with guarded and un-

guarded procedures against gravimetric results. The study has shown that better accuracy of corrosion estimation can be achieved with linear polarization resistance measurements performed without the guard ring (Liu and Weyers, 2003).

2.9 CORROSION TESTS

Assessing the corrosion of reinforcing steel bars embedded in concrete has some innate difficulties. The process of evaluating corrosion has difficulties, long-standing and conditional uncertainties. Dealing with slowness and variability of chloride and carbon-di-oxide penetration have always been a critical factor regarding those procedures. (Chappelow et al., 1992).

ASTM C 876 is a method to monitor the corrosion status of metal reinforcement in concrete. This method uses half-cell potential but nonfunctional at measuring corrosion rate. Also, this method is intended for use on the existing structure.

Researchers used different approaches to study the corrosion of reinforcement embedded in concrete. Some studies were performed in simulated concrete pore solution, and some studies try to derive pore solution from raw concrete and mortar sample. ASTM G 109 method is the only standard for evaluating the corrosion performance of reinforcement steel embedded in concrete; this uses half-cell and macro-cell measurement.

2.9.1 Accelerated Chloride Threshold Level Test

The critical chloride threshold of steel samples embedded in concrete is determined by the accelerated chloride threshold (ACT) test (Trejo and Miller 2003). Acceleration of chloride ions to the steel surface is done by this test. Chloride ions migrate under an electrical field's effect to the steel surface rather than slowly diffusing into concrete due to different concentrations.

3 x 6 in (75 x 150 mm) concrete cylinder made with steel reinforcement embedded in cylinders having attached chloride solution reservoirs at the top are used for ACT. The reservoirs are filled with 3.5% by weight of sodium chloride solution. A potential

difference of 20V need to apply for generating an electrical field between an anode at the reinforcement level and a cathode in the chloride reservoir. Negatively charged chlorides travel to the anode, and when they reach the chloride threshold level, after that corrosion initiate at the steel reinforcement. Corrosion of steel reinforcement is monitored through polarization resistance method. A reference electrode containing probe, which contains a reference electrode, named Haber-Luggin probe and a counter electrode are embedded in the mortar above the steel reinforcement to run the polarization resistance tests. Fig. 2.3 shows the layout of ACT test setup.

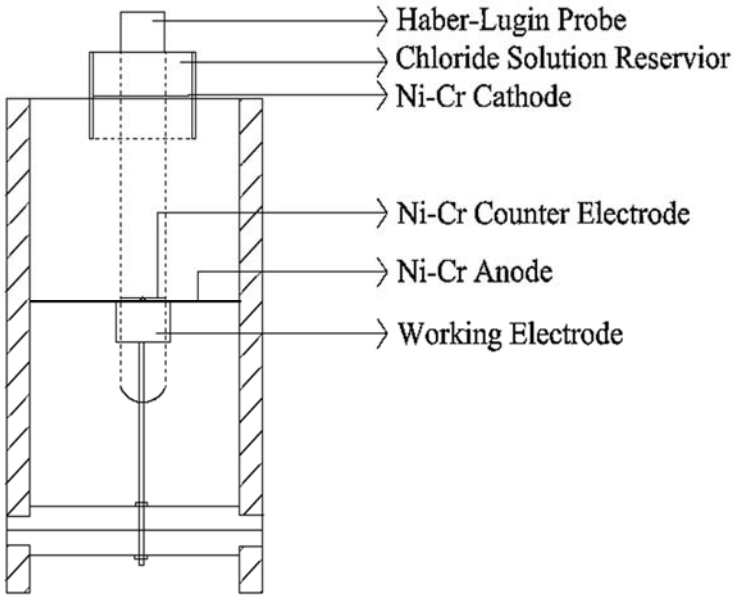

Fig. 2.3. ACT Test Layout.

An electrical field is applied in intervals of 6 hours, and polarization resistance of reinforcement is measured at the end of 42 hours waiting period. Testing ended when the initiation of corrosion is detected. The amount of chlorides at the steel reinforcement level is then measured to determine the chloride threshold value.

A similar chloride threshold measurement method has also developed by Castellote et al. (2002) that uses an electrical field to accelerate chloride ions transfer. This method monitors corrosion initiation through polarization resistance and uses mortar cubes with

embedded steel reinforcement. But the anode and the reference electrode are not embedded in the mortar. The anode is underneath the sample, and the cathode and the reference electrodes are placed in the chloride reservoir. Castellote et al. (2002) recommend using 10 to 13V potential difference to drive the chlorides and a 1M Sodium Chloride solution. Trejo and Pillai (2003) evaluated the use of 1, 5, 10, 20, and 40V potential differences for the electrical field. They determined that up to 10V the specimen's chloride profile development did not change notably.

Many researchers reported that chloride threshold levels change correspondingly with the environment's hydroxyl ion concentration. Glass and Buenfeld (1997) proposed to state chloride threshold levels as chloride to hydroxyl ratios. Trejo and Pillai (2003) reported that the pH of the environment around the reinforcement was decreasing with increasing magnitude of the applied electrical field and with increasing time of application due to the oxidation of hydroxyl ions at the anode. Similar to chlorides, negatively charged hydroxyl ions are also attracted to the anode. If their oxidation rate is higher than their percentage of transportation, the pH around the anode decreases. On the contrary, Castellote et al. (1999) recommended the addition of HCl to the chloride solution to neutralize the reinforcement environment. They suggested that the extra hydroxyl ions generated at the cathode by reducing water molecules were being attracted to the mortar, causing an increase in the pH of the environment. Due to their higher transference numbers, hydroxyl ions were also slowing the penetration rate of chlorides.

Castellote et al. (2002) used their chloride threshold determination method only with standard corrugated steel rebar embedded in the mortar with a water-cement ratio of 0.37. Still, they also tested some of their samples without an electrical field, where chlorides diffused into the mortar similar to longer-term standard corrosion tests. They covered that the accelerated test method results were identical to the results of the standard diffusion method. The accelerated test method's chloride threshold was 0.152% by weight of the sample and 0.227% by weight of sample for the diffusion method. Chloride thresholds expressed as chloride to hydroxyl ion ratio for the accelerated and diffusion tests were 2.0 and 1.5, respectively (Castellote et al., 2002). Viedma et al. (2006) also tested similar samples with a water-cement ratio of 0.45, using an electrical field to accelerate the

test and using the only diffusion of chlorides into the mortar. The chloride threshold for the embedded conventional corrugated steel rebar was 2 and 1.07 % by weight of cement for the diffusion and accelerated samples, respectively. Likewise, Castellote et al.'s results, the chloride threshold determined by the diffusion method was higher than the accelerated method. Corrosion initiation for the diffusion samples took 432 days, and the coefficient of variation of the results was 50%. For the accelerated samples, the initiation of corrosion took place at 1 to 6 days, and the variation coefficient was only 23%.

2.9.2 Rapid Macro-Cell Test

The rapid macro-cell test was developed at the University of Kansas under the Strategic Highway Research Program (Martinez et al., 1990). Two separate containers are filled with simulated concrete pore solution, reinforcing bars placed were between and intended to represent the top and bottom reinforcement mats of a bridge deck. Reinforcing bars were either exposed or overlaid with mortar. One container contains sodium chloride to initiate corrosion of reinforcing bars in that container (anode). The other container was supplied with scrubbed air for ensuring adequate oxygen supply necessary for reduction reactions (cathode). Reinforcing bars in separate containers were electrically connected across a resistor, and the solutions were connected over a salt bridge. The corrosion potential of reinforcing bars and the macro-cell current flowing between the containers through the resistor were monitored. Fig. 2.4 shows the test setup for the rapid macro-cell test.

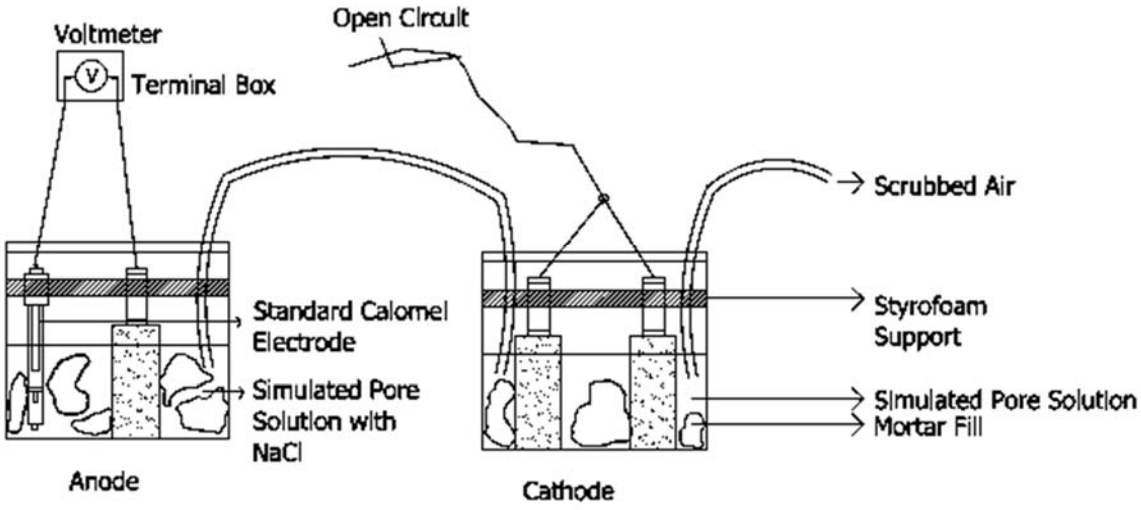

Fig. 2.4. Rapid Macro-Cell Test Setup

Several aspects of the test method such as the number and diameter of reinforcing bars in containers, the salt concentration in an anodic container, the magnitude of the resistor, and the height of solution were all altered by different researchers, who used this method in the following studies to improve the uniformity and repeatability of the results (Schwensen et al., 1995; Senecal et al., 1995; Smith et al., 1995). Reinforcing bars used in primary studies were only partially covered with mortar (lollipop samples), but later it was decided to insert the reinforcing bars entirely within the mortar (wrapped samples) to inhibit corrosion of reinforcing bars at the steel-mortar interface (Darwin et al., 2002).

Kahrs et al. (2001) applied the rapid macro-cell method to evaluate the corrosion performance of stainless steel clad bars. Different mortar cover thicknesses and different protection methods for the cut end of reinforcing bars were evaluated. The study also evaluated the corrosion potential and macro-cell current of sandblasted and damaged stainless steel clad samples. The research concluded that stainless steel bars have notable chloride corrosion resistance associated with conventional bars.

In another investigation, the rapid macro-cell method was used to assess the corrosion performance of micro-composite steel (MMFX) upon conventional steel and epoxy-coated reinforcement (Darwin et al., 2002; Gong et al., 2002). Mortar wrapped

conventional steel, MMFX steel, and epoxy coated steel samples were exposed to 1.6 molal chloride solution for 15 weeks. Epoxy coated bars were combined with uncoated bars as cathodes, and the study also evaluated successions of MMFX steel and conventional steel. In addition to rapid macro-cell tests, the reinforcing bars were also tested with the cracked beam test method and southern exposure method, which need more time to initiate when compared to the rapid macro-cell method. Results indicated that MMFX steel performed better than conventional steel samples and more acute than epoxy coated samples. The results of the rapid macro-cell tests and the long-term bench-scale tests (southern exposure test and cracked beam test) were in good agreement. Results also indicated that combining MMFX steel with conventional steel reduced the corrosion performance of MMFX steel.

In 2005, Balma et al. used the rapid macro-cell test method in addition to southern exposure and cracked beam tests to evaluate different corrosion protection systems, such as different water-cement ratios, corrosion inhibitors, and different steel types. Three different micro-alloyed thermex treated steels, thermex treated conventional steel, MMFX micro composite steel, epoxy-coated steel, pair of duplex steels, and uncoated normalized steel were evaluated for corrosion performance applying rapid macro-cell. Corrosion potential and corrosion rates were monitored. Total corrosion loss of samples was lower in mortar and concrete with lower water-cement ratios and in mortar and concrete containing corrosion inhibitors. Reinforcing bar coated with epoxy resin showed lower corrosion loss associated with traditional bars. The investigation further indicated that the correlation of total corrosion loss achieved from rapid macro-cell corrosion test, southern exposure test, and the cracked beam test was good in most situations and had related variability.

Gong et al. (2006) also used the rapid macro-cell test to evaluate the effectiveness of different corrosion inhibitors and different steel types to decrease corrosion. In addition to rapid macro-cell tests, bench-scale tests such as southern exposure test, cracked beam test, and ASTM G 109 tests were performed. The study evaluated conventional epoxy-coated reinforcing bars, stainless steel 316LN clad bars, different corrosion inhibitors, bars coated with conventional epoxy over a primer coat that containing calcium nitrite, adhesion epoxy-coated bar, and galvanized bars with blue epoxy coating. Linear polarization tests were also performed on bench-scale test specimens to estimate micro-cell corrosion.

Results showed that stainless steel clad reinforcement exhibited higher corrosion performance if the cladding was not damaged related to conventional reinforcement and epoxy-coated reinforcement. Finding of this study was that the measured micro-cell corrosion rates for conventional steel samples in southern exposure and ASTM G 109 samples were one order of magnitude higher compared to the macro-cell corrosion rates.

Guo et al. (2006) performed very similar research with different epoxy coated reinforcements and other corrosion protection systems using the rapid macro-cell test, southern exposure test, cracked beam test, and ASTM G 109 test. The results of the study were very similar to the results of Gong's study (Gong et al., 2006). However, there were a couple of contradicting results. The results of this study indicated that the corrosion performance of epoxy-coated reinforcing bars with primer containing calcium nitrate improved for un-cracked samples with a water-cement ratio of 0.35 compared to conventional steel samples. Gong et al. noted that there was no significant improvement in their corrosion performance. Guo et al. (2006) also showed that, although there was a good correlation between the results of the rapid macro-cell test and bench-scale tests, the rapid macro-cell test was better in recognizing differences among corrosion protection schemes.

2.9.3 Chloride Ion Threshold Test

Chloride ion threshold test method is being developed to enhance the existing protocol ASTM G 109 and is focusing on chloride ion threshold measurement to assess the effectiveness of various corrosion protection systems, such as admixtures (Berke et al. 2003). The recommended test method requires the placement of two reinforcement bars at two layers in cylindrical test units that are cast using a standard mortar mixture. The only modification allowed to the standard mortar is the incorporation of the material being evaluated. Specimens are moist cured and dried at a standard laboratory conditions before they are exposed to cyclic wetting and drying with a chloride solution. Macro-cell current flowing among the two layers of reinforcement over a 10-ohm (Ω) resistor, open circuit potential of the top reinforcement, and the linear polarization resistance of the top

reinforcement are monitored throughout the test to determine the initiation of corrosion. Testing of samples is stopped, and the chloride ion content at the top reinforcement level is determined when all of the electrochemical measurements indicate corrosion initiation for two sequential weeks. The draft standard for this test states that the method is intended to evaluate the comparative representation of corrosion protection schemes and that the measured results do not interpret to corrosion rates transpiring in structures. Fig. 2.5 shows the test setup for chloride ion threshold.

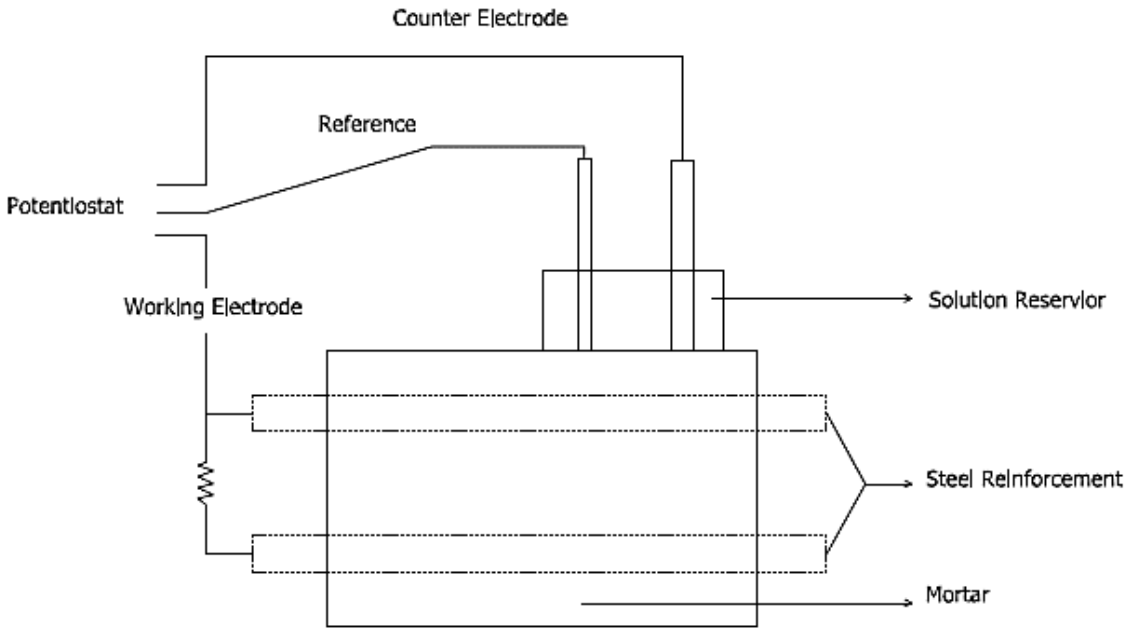

Fig. 2.5. Chloride Ion Threshold Test Layout

2.9.4 ASTM G 109 and Modified G 109 Test

ASTM G 109 is a broadly used standard in corrosion studies to evaluate many corrosion protection methods, including various concrete properties, supplementary cementing materials, corrosion inhibitors, and corrosion-resistant reinforcement steels. The

method uses 11 x 6 x 4.5 in concrete samples with two layers of reinforcement. The top layer consists of one reinforcing bar with a 0.75 in (19 mm) concrete cover and two bottom layer bars. The two layers of reinforcement are electrically connected over a 100 Ω resistor. The samples are ponded with a sodium chloride solution for two weeks and kept dry for two weeks. Macro-cell corrosion current and the half-cell potential of the bars against a CSE reference electrode are monitored. ASTM committee G 01 has performed an inter-laboratory and intra-laboratory study for the ASTM G 109 method and reported that the top end of the 95% confidence interval for time to failure for control specimens with 0.75 in (19 mm) cover was six months for both inter and intra laboratory tests.

This inspection process has been widely used by many researchers to evaluate different corrosion protection methods, and many modifications of it were executed. The number of bars at the top and bottom layer, the magnitude of the resistor between the layers, chloride concentration of ponding solution, wetting and drying cycles were all revised by different researchers. Although the standard notes that the time to failure is six months, the literature indicates that this time is much longer.

2.10. Causes of Corrosion in Reinforcement

Corrosion of the steel reinforcement bars may occur due to localized failure of the passive film on the steel by chloride ions or a general failure of the passivity by neutralization of the concrete due to reaction with carbon dioxide from the atmosphere. The main factors responsible for corrosion of reinforcement bars are:

1. **Loss of alkalinity due to carbonation**: When the steel surface is left unprotected in the atmosphere, rust begins to form on the steel surface and gradually flakes off.

2. **Loss of alkalinity due to chlorides**: Chloride ions tend to de-passivate the steel surface by destroying the alkalinity of the concrete.

3. **Cracks in concrete**: Cracks may expose the steel bars to the atmosphere and hence increase carbonation.

4. **Moisture pathways**: Regular wetting of the concrete may lead to water reaching the steel reinforcement bars by diffusion through the pore structure of the concrete or cracks present in the concrete. Rusting of the steel bars follow thereafter.

5. **Insufficient Cover:** Insufficient dimension of concrete cover.

2.11. Effects of Corrosion on Steel Bars

Once the steel bars start corroding, the reinforced concrete member gradually begins deteriorating going through the following stages:

1. **Formation of white patches:** Atmospheric carbon dioxide reacts with calcium hydroxide present in the cement paste forming calcium carbonate. This calcium carbonate is carried by moisture and deposited onto the concrete surface forming white patches.

2. **Brown patches along reinforcement:** When the steel bars start corroding, a layer of iron oxide is formed on it. This iron oxide also gets carried to the surface of the concrete by moisture.

3. **Formation of cracks:** The products of corrosion occupy a greater volume than the original material. Hence they exert pressure on the concrete and crack it. With more corrosion occurring, more and wider cracks are formed.

4. **Spalling of concrete cover:** Due to loss of the bond between concrete and steel, the concrete starts forming multiple layers of scales and peels off. The steel bars also get reduced in size.

5. **Snapping of bars:** Due to reduction in the size of the steel bars, they finally snap. Also, there is a considerable reduction in the size of the main bars.

6. **Buckling of bars:** Spalling of the concrete cover and snapping of bars lead to buckling of the main bars. This bulges the concrete in that region and eventually the whole structure collapses.

2.12. Corrosion Protection Measures

Corrosion of steel reinforcement bars may be prevented or at least delayed by practicing good measures. Also, damaged steel bars can be repaired and the concrete structure can be restored properly. Some steps are given below:

1. **Providing Sufficient Concrete Cover:** A good amount of concrete cover should be provided over the steel reinforcement bars. This ensures proper maintenance of the alkaline nature within the concrete and the passivity of the steel bars. The steel bars should be precisely placed in position

2. **Use of Good Quality Concrete:** High quality concrete must be used. It helps to maintain proper alkaline nature. For the concrete, a water/cement ratio of 0.4 or less is to be maintained. Excessive water may damage the steel bars.

3. **Proper Compaction of Concrete:** Concrete must be completely compacted such that there are no air voids or pockets present inside.

4. **Use of FBE coated Bars:** Fusion Bonded Epoxy Coating (FBEC) may be applied on the steel bars to prevent them from corrosion.

5. **Use of Cement Based Polymers:** Cement based polymers can be used in the concrete to enhance its protection against corrosion capabilities. The cement based polymers act

as a binder in the concrete. They also increase the durability, tensile strength and vibration damping of the concrete

6. **RCPT test to assess degree of Corrosion:** The Rapid Chloride Permeability Test (RCPT) may be performed to assess the degree of corrosion. The quantity of electrical current that passes through a sample 50 mm thick and 100 mm in diameter in 6 hours is measured. Based on this a qualitative rating is made of the permeability of the concrete

2.13. Previous Studies on Application of Epoxy Coated Reinforcement

Epoxy-coated reinforcement (ECR) is used in many bridges in the U.S. ECR is produced by applying epoxy powder on freshly blasted steel surfaces at high temperatures. Reinforcing bars covered with melted epoxy are quenched, usually in a water spray bath. Although ECR has been commonly used since the 1970s in bridge decks, recent studies reported that ECR may not provide the desired service life due to cathodic disbondment problems. Florida Department of Transportation study stated that electrochemical disbondment of epoxy coatings could initiate due to exposure to salt water and subsequent macro-cell corrosion during service in bridge substructures (Sagues et al., 1994). However, later studies of cathodic disbondment of epoxy coated bars reported that the adhesion reduction was related to water penetrating the coating and oxidation of the underlying steel, rather than the presence of the chloride ions or excessive coating damage (CRSI 1995; Weyers et al., 1998). If the coating had already disbonded when chloride ions arrived at the surface of the reinforcement, corrosion could occur under the coating (Pyc et al., 2000).

Although cathodic disbondment of ECR was reported by many researchers, a study performed in 1996 reported that ECR incorporating reinforced concrete structures performed well. The study evaluated a total of 92 bridge decks, two bridge barrier walls, and one noise barrier wall located in 11 states and three provinces that were built with ECR and found that overall, the structures were in good condition, and only two percent of

evaluated ECR segments exhibited significant corrosion. These were extracted from locations of heavy cracking, shallow concrete cover, high concrete permeability, and high chloride concentrations (Smith and Virmani, 1996). In another study it was reported that to get the best performance from epoxy coated bar, it should be used not only for the top mat but for both top and bottom mats. The study also recommended the repair of cracks and damaged areas of epoxy coated epoxy coated reinforcements (McDonald et al., 1998).

2.14 Concrete as a Structural Material

Concrete is used widely in building and other civil engineering structures, due to its low cost, flexibility, durability, and high strength. It also has high resistance to fire. Concrete is a non-linear, non-elastic and brittle material. It is strong in compression and very weak in tension. It behaves non-linearly at all times. Because it has essentially zero strength in tension, it is almost always used as reinforced concrete, a composite material. It is a mixture of sand, aggregate, cement and water. It is placed in a mold, or form, as a liquid, and then it sets due to a chemical reaction between the water and cement. Concrete is any product made by the use of cementing medium. This medium is mainly the product of reaction between hydraulic cement and water (Neville and Brooks, 2010). In the general case binder component, which can be in hard crystalline or amorphous state is considered as the matrix of composite material. The term structural concrete indicates all types of concrete used in structural applications (Hassoun and Al-Manaseer, 2008).When aggregate is mixed with dry cement and water, the mixture forms a fluid slurry and forms a hard matrix that binds the materials together into a durable stone-like material that has many uses (Li, 2011). Often, additives such as pozzolans or superplasticizers are included in the mixture to improve the physical properties of the wet mix or the finished material. Most concrete is poured with reinforcing materials such as rebar embedded to provide tensile strength, yielding reinforced concrete.

2.15. Aggregate in Concrete as a Constituent

Concrete is a mixture of cementous material, aggregate, and water. Aggregate is commonly considered inert filler, which accounts for 60 to 80 percent of the volume and 70 to 85 percent of the weight of concrete (Neville and Brooks, 2010). Although aggregate is considered inert filler, it is a necessary component that defines the concrete's thermal and elastic properties and dimensional stability. Aggregate is classified as two different types, coarse and fine. Coarse aggregate is usually greater than 4.75 mm (retained on a No. 4 sieve), while fine aggregate is less than 4.75 mm (passing the No. 4 sieve). Coarse aggregates are usually obtained from natural rocks, either crushed stones or natural gravels, and fine aggregates are usually river sand. Water is added in the mix to initiate the binding process, as cement is a hydraulic material which gives strength once it starts reacting with this mixing water. Not only may the aggregate limit the strength of concrete, but the aggregate properties greatly affect the durability and structural performance of concrete. Aggregate was originally viewed as an inert, inexpensive material dispersed throughout the cement paste so as to produce a large volume of concrete. Not only may the aggregate limit the strength of concrete, but the properties of aggregate greatly affect the durability and structural performance of concrete (Neville, 2011). Although aggregates are most commonly known to be inert filler in concrete, the different properties of aggregate have a large impact on the strength, durability, workability, and economy of concrete. These different properties of aggregate allow designers and contractors the most flexibility to meet their design and construction requirements.

2.16. General Classification of Aggregate

Aggregates can be classified based on their origin. Aggregates can come from natural sources, or may be derived from industrial by-products. Natural aggregates may be basalt, granite, limestone, quartzite, schist, shingles, etc.; whereas, industrial aggregates can be made from bricks, iron slag, plastic, or recycled concrete as aggregate. But, aggregates are usually classified based on their particle size. Aggregates passing through

ASTM #4 sieves (4.75 mm) are termed as fine aggregate, while those retained on the sieve are termed as coarse aggregate.

2.17. Aggregates Commonly Used in Bangladesh

In Bangladesh, brick chips, crushed stone, shingles, jhama bricks are commonly used as coarse aggregate in construction. Bangladesh is the largest delta in the world. Due to its geographical condition availability of stone aggregate is very limited in Bangladesh. Generally in the construction field clay burnt bricks are used as coarse aggregate.

Concrete is one of the maximum extensively used production substances in the world. However, the manufacturing of Portland cement is an important constituent of concrete which results in the discharge of huge quantities of CO_2 and greenhouse gases. Manufacturing of 1 ton of Portland cement produces approximately one ton of CO_2 and different greenhouse gases. Along with environmental issues, the natural resources which are used as raw materials for the production of concrete are also limited. If the supply of limestone in a particular region gets stopped there will not be possible to produce Portland cement and the associated cement companies will not be functional anymore. That's why sustainability in concrete production is now a very important issue for many researchers to safeguard the environment and for the betterment of mankind. Researchers are producing research results for utilizing recycled aggregate as coarse and fine aggregates considering physical and mechanical properties of aggregate, fresh properties of concrete made with recycled aggregate, durability properties, etc. Considering the outputs of the research findings; guideline for utilization of recycled aggregate has been approved in many countries. Still many researchers are working on recycled aggregates to use them in the construction works to make sustainable development.

Mohammed et al. (2007) has made tremendous researches on many aspects related to sustainability of construction materials in Bangladesh. Different important factors of deterioration of existing concrete structures in Bangladesh were studied (Mohammed et al., 2013). Extensive investigations were carried out on recycling of concrete made with brick

aggregate since 2004 (Mohammed et al., 2015). As per study Mohammed et al. (2011) conducted that concrete made with recycled brick aggregate can produced similar amount of compressive strength of concrete made with stone aggregate when abrasion value of recycled brick aggregate matches with that of stone aggregate. As per the investigation of Mohammed et al. (2014), the average strength of concrete made with RBA was found to be 25 MPa and 21 MPa for w/c = 0.45, and w/c = 0.55 respectively. These results signifies that RBA can be used for making structural grade concrete as per ACI 318-19 because as per ACI 318-19, the minimum strength of structural grade concrete is specified to be 21 MPa (ACI 318-19, 2019).

Separate studies were also conducted on shear and flexural strength of reinforced concrete beams made with RBA and it was evaluated that ACI 318 provisions can be used for flexural and shear designs of reinforced concrete beams made with RBA (Mohammed et al., 2019).

In this study high emphasis has been given to evaluate the effect of chloride ingress, micro-cell and macro-cell corrosion propagation for concrete made with recycled brick aggregate along with stone and virgin brick aggregate. Many studies have already been done considering stone and virgin brick aggregate for corrosion and chloride penetration investigation. But previously no study has been done considering recycled brick aggregate both as coarse and fine aggregate which has made this research very unique.

2.18 Research Gaps of Past Studies on Chloride Ingress and Corrosion of Steel Bars

Many studies have already been conducted regarding corrosion mechanisms and chloride ingress in concrete. Corrosion at un-cracked concrete has been described by Mohammed et al. (2003) considering both short-term laboratory tests and long-term marine exposure tests. Mohammed et al. (2003), Arya and Ofori-Darko (1996) have already investigated corrosion mechanisms at cracked concrete. Corrosion of cement paste coated steel bars already have been conducted by Mohammed et al. (2003). But no detailed study

has been conducted on corrosion in reinforced concrete considering different aggreates used in Bangladesh. With this background the study has been planned to evaluate chloride ingress and corrosion of steel bars in reinforced concrete made with different aggregates.

Detailed investigation on macro-cell and micro-cell corrosion of steel bars in cracked concrete under marine environment was conducted by Mohammed et al. (2001). In his study he investigated total 6 cases having two types of cements; normal portland cement (NPC) and slag cement of type B (SCB: NPC 55% and Slag 45%) with varying stress level imposed to specimens. He investigated corresponding compressive strength, half cell potential, macro-cell corrosion, micro-cell corrosion, chloride concentration, SEM , XRD testings along with various visual observations. He found in his investigation that immediately after exposure in marine environment, a significant amount of macro-cell corrosion was formed over the steel bars located near the cracked region and the amount of corrosion got decreased eventually due formation of rust layer and healing of cracks with $CaCO_3$, $Mg(OH)_2$, ettrigite and rust. He found that though the micro-cell corrosion was very low at the early age, it got increased gradually and exceeded the amount of macro-cell corrosion later. He divided full corroion progress into macro-cell dominationg early stage and micro-cell governig later stage. But still effects of aggregates on macro-cell and micro-cell corrosion were missing in the study.

Mohammed et al. (2004) made long term exposure investigation keeping the specimens at tidal pool for 15 years to evaluate both micro-cell and macro-cell corrosion of steel bars of cracked concrete made with different types of cements. The types of cements that he used for this study were ordinary portland cement (OPC) , slag cement of types A (SCA), B (SCB) and C (SCC); and fly ash cement of Type B (FACB). Water to cement ratios were 0.45 and 0.55. As per the observed data he proposed a relationship between macro-cell corrosion and micro-cell corrsion, and three other ralations between pit depth and crack widths for both tidal and submerged exposures. In the investigation it was found that dense microstructure of concrete made with large amount of slag (SCN, SCC) caused maximum accumulation of chloride at the vicinity of unhealed wider cracks.

But still chloride ingress rate and corroion effects for splash zone condition were missing in the study.

Andrade et al. (1992) had analyzed the relative contributions of macro-cell and micro-cell corrosion. They concluded that the influence of the macro-cell corrosion only became significant when the ratio of surface areas of the passive or active regions is greater than approximately 50:1. Moreover, it was obserevd that the theoritical maximum effect (with an infinitively large cathode and infinitively small anode) would be an increase in an active corrosion rate of only 2-5 times that of the micro-cells alone. In this study no investigation was conducted on the influence of cement and aggregates types on corrosion propagations.

Hansson et al. (2006) had investigated about the macro-cell and micro-cell corrosion of steel bars for the effects of corrosion for ordinary portland cement and high performance concrete. The corrosion investigation was continued for 180 weeks and special ponding well was established on the top of every speciemns with 3% NaCl solution. As per their investigation they observed that the total corrosion rate was approximately three times that of micro-cell corrosion alone. For having lower diffusion rate high performance concrete (HPC) showed one order lower rate of corrosion than the steel bars embabed in concrete made with ordinary portland cement (OPC). No investigation was conducted regarding chloride ingress and infulence of aggregates for the formation of corrosion.

Feng et al. (2011) studied about the chloride induced corrosion in reinforcement in cracked concrete beams. In his study he used C30 ordinary Portland cement (OPC) as binding material, crushed gravel as coarse aggregate, natural sand as fine aggregate and made five 150 x 180 x 1000 mm sized concrete beams as specimens. Rapid chloride penetration test (RCPT) was conducted for determination of chloride ion content. He established a model of equivalent chloride diffusion coefficient related with crack width. He also showed that equivalent chloride diffusion coefficient increased with the increase of crack width. He concluded that when the crack width is 0.1 mm to 0.3 mm the increase factor for chloride induced corrosion remains steady but when the crack width is more than

0.3 mm the factor got increased accordingly. This study was only limited to chloride penetration rate for different crack widths.

Mohammed et al. (2003) studied about micro-cell and macro-cell corrosion of steel bars in cracked concrete under marine environment. For this investigation he used single cracked 60 cm x 10 cm x 10 cm sized prism specimens with W/C ratio of 0.40, 0.45, and 0.50 with rounded 9 mm deformed bar as reinforcement embedded inside. For mix design ordinary Portland cement, slag cement of types A, B & C, fly ash cement of type B, natural river sand as fine aggregate, crushed granite as coarse aggregate were used. Test on compressive strength, debonded area, half-cell potential, macro-cell corrosion, micro-cell corrosion, oxygen permeability, chloride-ion concentration, weight loss of steel elements were investigated very carefully in this research work. He concluded that w/c ratio had high effects on macro-cell and micro-cell corrosion rates. He found that narrower cracks got naturally filled in long term exposure conditions and corrosion amount got reduced accordingly. The unhealed cracks were found to generate higher corrosion rate forming deeper pits. He also concluded that cracks as well as voids at the steel concrete interface were responsible for deeper corrosion pits. In this study effects of different aggregates for corrosion formation was missing.

Ramezanianpour et al. (2018) modelled chloride ions penetration in cracked concrete structures. Specimens of this investigation were subjected to tidal zone of Persian Gulf for 48 months. Both cracked and un-cracked specimens were investigated. In his experiment electrical resistivity, half-cell potential, corrosion current density, water absorption, crack width and crack depth were measured. As per experimental results he concluded that with the increase of crack width corrosion rate got increased. Pozzolanic materials such as Silica fume proved to help in reducing crack depth. An equation establishing relation between crack width and crack depth was also established. In this study also effects of different aggregates for corrosion formation was missing.

Mohammed et al. (2013) in his another study made detailed experiment about the performance of different cement paste coated steel bars against chloride induced corrosion. For this experiment he used Normal Portland Cement (NPC), crushed granite as coarse

aggregate and river sand as fine aggregate with w/c ratio of 0.50. Test items included compressive strength of concrete, acid soluble and water soluble chloride ingress, half-cell potential, polarization resistance of steel bars, concrete resistance, anodic polarization curves, microscopic investigations on steel concrete interface, physical evaluation of corrosion such as corroded area, pit depth, weight loss etc. Using dense cement paste with lower W/C ratio was proven to reduce chloride ingress. Alumina cement paste coating found to produce porous interface. He concluded that cement paste coated steel bars should be used for sustainable marine reinforced structures. A relationship between water soluble and acid soluble chloride concentration was also established indicating that water soluble chloride concentration amounts 0.708 times of acid soluble chloride concentration. In this study effects of different aggregates for corrosion formation was missing.

In all the above mentioned studies mainly corrosion mechanisms for the steel bars embedded inside concrete and corresponding chloride ingress were evaluated for different types of cements, exposure conditions, crack widths and many other factors. But still extensive studies on corrosion and chloride ingress for different types of aggregates commonly used in Bangladesh such as fresh brick aggregate, stone aggregate and recycled brick aggregate need to be conducted. On this background this study was planned.

CHAPTER 3: EXPERIMENTAL METHOD

3.1 Introduction

In this chapter, the experimental method of the study is summarized. It includes the mixture proportions of concrete, cases investigated in the study, collection and preparation of materials, material properties, experimental setup, sample preparation, curing, reinforcement preparation steps and various testing procedures such as compressive strength, chloride ingress in concrete, macro-cell and micro-cell corrosion, half-cell potential, concrete resistance, physical evaluations of the reinforcements.

3.2 Collection of Materials

The types of coarse aggregate that were used for this investigation were fresh brick aggregate (BA), recycled brick aggregate (RBA) and stone aggregate (SA). RBA was collected from a 15 year old demolished building located at Tongi, Dhaka. As fine aggregate, natural river sand (NS) was used. Concrete samples were also made with recycled brick fine aggregate (RBFA). The fineness modulus (FM) of natural river sand and recycled fine brick aggregate was 2.7 and 3.15 respectively. The fineness modulus of coarse aggregates was 6.6 for all coarse aggregates. As binding material CEM Type -1 as per BDS EN-197 (95% clinker plus 5% other minor constituents) was used. 10 mm diameter Grade 500W (produced as per ASTM A706, yield strength = 540 MPa, ultimate strength = 660 MPa, % elongation = 21.5) steel bars were used for investigation of macro-cell corrosion over the steel bars in concrete. Some specimens were also made with epoxy coated steel bars. As mixing water of concrete, potable tap water was used. For sea water exposure, sea water was collected from the Bay of Bengal.

Fig. 3.1. Site at Tongi for Collecting RBA

3.3 Material Properties

The properties of materials used were evaluated before casting by testing them in the laboratory according to specifications. The aggregates used in this study were tested for specific gravity, absorption capacity, fineness modulus, abrasion resistance, gradation, and unit weight. The specifications followed are summarized in Table 3.1.

Table 3.1. Specifications Followed to Test Material Properties

Name of the Property Evaluated	Specification/Guideline Followed
Specific Gravity	ASTM C 127 (For Coarse Aggregate) ASTM C 128 (For Fine Aggregate)
Absorption Capacity	ASTM C 127 (For Coarse Aggregate) ASTM C 128 (For Fine Aggregate)
Abrasion Resistance	ASTM C 131
Unit Weight	ASTM C 29
Gradation	ASTM C 33
Fineness Modulus	ASTM C 136

3.3.1 Coarse Aggregate

For this investigation, three types of coarse aggregates were used. They were virgin brick aggregate (BA), recycled brick aggregate (RBA) and stone aggregate (SA). The gradation of coarse aggregates followed in this study is as per ASTM C33. The gradation of coarse aggregate and material properties are summarized in Table 3.2. and Table 3.3. accordingly.

Table 3.2. Gradation of Coarse Aggregate (According to ASTM C33)

Nominal Size	Amounts Finer than Each Laboratory Sieve, Mass Percent				
	19.0 mm	12.5 mm	9.5 mm	4.75 mm	2.39 mm
25 to 12.5 mm	95	-	37.5	5	-

Table 3.3. Properties of Coarse Aggregate

Type of Coarse Aggregate	Specific Gravity	Absorption Capacity (%)	Abrasion (%)	SSD Unit Weight (kg/m^3)	Fineness Modulus
BA	2.2	21.1	47	1321	Controlled as per ASTM C 33 – 03
SA	2.65	2.9	25	1550	
RBA	2.14	12.4	43	1227	

3.3.2 Fine Aggregate

For this study, natural river sand (NS) was used as fine aggregate. Concrete samples were also made with recycled fine aggregate (RBA). Prior to casting the fine aggregates were tested for specific gravity, absorption capacity, unit weight and fineness modulus (FM). The material properties of fine aggregates are summarized in Table 3.4. Both fine aggregates satisfy ASTM C 33 specification, as shown in Fig. 3.2. and Fig. 3.3.

Table 3.4. Properties of Fine Aggregate

Aggregate Type	Specific Gravity	Absorption Capacity (%)	SSD Unit Weight (kg/m3)	Fineness Modulus
NS	2.6	3.9	1575	2.7
RBA	2.1	10.7	1415	3.15

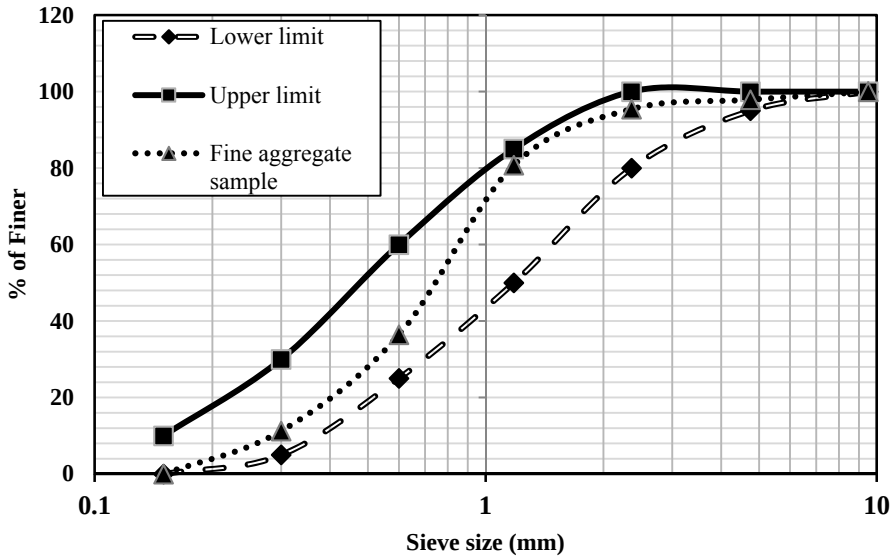

Fig. 3.2. Aggregate Gradation Curve for NS

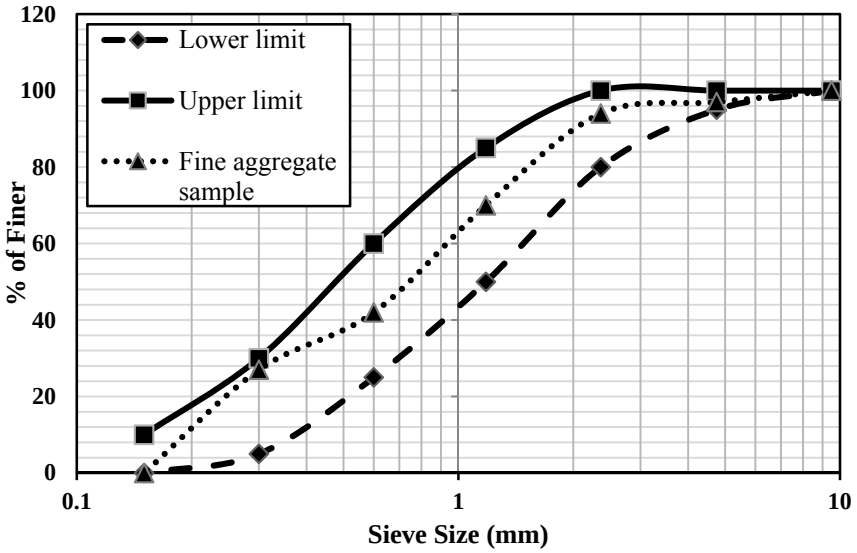

Fig. 3.3. Aggregate Gradation Curve for RBFA

3.3.3 Cement

As binding material CEM Type I (Ordinary Portland Cement (OPC)) was used in this study that conforms to BDS EN 197 – 1: 2000, and ASTM C595. The composition of the mineral components is given in Table 3.5 (as specified by the manufacturer). The principal raw materials used in the manufacture of Ordinary Portland Cement are:

1. Argillaceous or silicates of alumina in the form of clays and shales.
2. Calcareous or calcium carbonate, in the form of limestone, chalk and marl which is a mixture of clay and calcium carbonate.

Table 3.5. Mineral Composition of OPC

Component	Percentage
Clinker	95~100%
Slag, Fly Ash, and Limestone	0 %
Gypsum	0–5%

3.3.4 Water

Water used in this study for concrete mixing and curing was potable tap water whose unit weight was 1000 kg/m^3. This was free from any detrimental contaminants and was good potable quality.

3.3.5 Reinforcement

10 mm diameter Grade 500W (produced as per ASTM A706, yield strength =500 MPa, ultimate strength = 660 MPa, % elongation =21.5) steel bars were used for investigation of macro-cell corrosion over the steel bars in concrete. Some specimens were also made with epoxy coated steel bars. The chemical composition of steel bars is shown in Table 3.6.

Table 3.6. Chemical Composition of Reinforcement

Component	C	Mn	Si	S	P
Percentage (%)	0.21	0.67	0.17	0.028	0.035

3.4 Cases Investigated

For this experiment total 16 separate cases were investigated. Case variations were made by different types of coarse aggregates (RBA, SA, BA), cement contents (340 and 400 kg/m^3), W/C ratios (0.45 and 0.50), fine aggregate (NS and RBFA) and rebar types (deformed bar and epoxy coated bar) used. Details of 16 cases are shown on Table 3.7.

Table 3.7. Cases Studied

Case	Cement Content (kg/m^3)	W/C	CA	FA	Cement Type	Rebar Type	Case Identification
C1	340	0.45	RBA	NS	OPC	Deformed	RBA-NS-0.45-340
C2	400	0.45	RBA	NS	OPC	Deformed	RBA-NS-0.45-400
C3	340	0.55	RBA	NS	OPC	Deformed	RBA-NS-0.55-340
C4	400	0.55	RBA	NS	OPC	Deformed	RBA-NS-0.55-400
C5	340	0.45	SA	NS	OPC	Deformed	SA-NS-0.45-340
C6	400	0.45	SA	NS	OPC	Deformed	SA-NS-0.45-400
C7	340	0.55	SA	NS	OPC	Deformed	SA-NS-0.55-340
C8	400	0.55	SA	NS	OPC	Deformed	SA-NS-0.55-400
C9	340	0.45	BA	NS	OPC	Deformed	BA-NS-0.45-340
C10	400	0.45	BA	NS	OPC	Deformed	BA-NS-0.45-400
C11	340	0.55	BA	NS	OPC	Deformed	BA-NS-0.55-340
C12	400	0.55	BA	NS	OPC	Deformed	BA-NS-0.55-400
C13	340	0.45	RBA	RBFA	OPC	Deformed	RBA-RBFA-0.45-340
C14	400	0.45	RBA	RBFA	OPC	Deformed	RBA-RBFA-0.45-400
C15	340	0.55	RBA	RBFA	OPC	Epoxy coated	RBA-RBFA-0.55-340-E
C16	400	0.55	SA	NS	OPC	Epoxy coated	SA-NS-0.55-400-E

Note: CA, FA, RBA, SA, BA, NS, RBFA and E represent coarse aggregate, fine aggregate, recycled brick aggregate, stone aggregate, brick aggregate, natural river, recycled brick fine aggregate and fusion bonded epoxy coated bar respectively.

3.5 Concrete Mixture Designs

The mix proportion used in this study was done on weight basis and the unit contents of the ingredients of concrete were assumed to sum up to 1 m^3 of concrete and can be correlated by the following equation:

$$\frac{C}{G_c Y_w} + \frac{S}{G_s Y_w} + \frac{A}{G_A Y_w} + \frac{W}{G_w Y_w} + \frac{Air(\%)}{100} = 1 \quad (3.1)$$

Where,

C = Unit content of cement (kg/m^3 of concrete)

S = Unit content of fine aggregate (kg/m^3 of concrete)

A = Unit content of coarse aggregate (kg/m^3 of concrete)

W = Unit content of water (kg/m^3 of concrete)

γ_w = Unit weight of water (kg/m^3)

G_c= Specific gravity of cement

G_s = Specific gravity of fine aggregate (SSD)

G_A = Specific gravity of coarse aggregate (SSD)

G_w = Specific gravity of water

Air (%) = Percentage of air in concrete (assumed at 2% without air entraining agent)

All the mix designs of 16 cases are shown on Table 3.8.

Table 3.8. Mix Designs of All the Cases

Case	G_{max} (mm)	W/C	S/a %	C (kg/m^3)	W kg/m^3	S kg/m^3	G kg/m^3
C1	20	0.45	44	340	153	780	836
C2	20	0.45	44	400	180	729	782
C3	20	0.55	44	340	187	743	797
C4	20	0.55	44	400	220	686	736
C5	20	0.45	44	340	153	780	1141
C6	20	0.45	44	400	180	729	1067
C7	20	0.55	44	340	187	743	1087
C8	20	0.55	44	400	220	686	1003
C9	20	0.45	44	340	153	780	872
C10	20	0.45	44	400	180	729	816
C11	20	0.55	44	340	187	743	831
C12	20	0.55	44	400	220	686	767
C13	20	0.45	44	340	153	594	836
C14	20	0.45	44	400	180	556	782
C15	20	0.55	44	340	187	566	797
C16	20	0.55	44	400	220	686	1003

Note: W, C, G, S, and a represent water, cement, gravel, sand, and aggregate (coarse and fine), respectively. RBA, SA, BA, and NS represent recycled brick aggregate, stone aggregate, brick aggregate, and natural river sand respectively.

3.6 Reinforcement Preparation

Before casting, the materials were prepared to satisfy the specifications of ASTM C 39 (2003). For reinforced specimens, huge reinforcement preparation such as cutting and drilling of rebar, immersing rebars at solution, cleaning rebars using wire mesh, measuring weight and length of bars, connecting electric cables with rabars, connection testing using

multi-meter, adding epoxy gum to end of rebar, final washing of steel surface using Acetone solution etc. were done prior to casting work. Then on the basis of the mix design shown on Table 3.8. all the aggregates were separated. Prior to casting, both coarse and fine aggregates were brought to a saturated surface dry (SSD) condition to ensure that the w/c ratio of the mix remained as specified by the mixture proportion. The w/c ratio of the mix was monitored carefully.

For this investigation 10 mm diameter deformed bars and epoxy coated bars were collected from BSRM. The steel bars were cut into three specific size pieces of 5 cm, 13.5 cm and 34 cm. Reinforcements were submerged in 10% Diammonium Hydrogen Phosphate solution for 24 hours before casting and were rubbed with wire mesh to remove the reinforcements from existing rusts before being placed into concrete. After preparation of steel bars necessary works for electrical connections were done and associated equipment and materials were readied before each casting work. Materials related with electrical connections were electric cables with three colors red, black and yellow, soldering iron, Aluminium coil for soldering work, epoxy gum etc. Reinforcement is prone to corrosion as it gets surrounded by oxygen and humidity which enables the corrosion reaction to be happened consequently. So just before casting work all the preparation works of reinforcement were done carefully. Reinforcement preparation was a very important part of this investigation. Following are the steps of reinforcement preparation described shortly:

a) Cutting and Drilling of Rebar

The 10 mm diameter steel bars which were collected for this investigation were cut into three specific sizes of 5 cm, 13.5 cm and 34 cm. After cutting the steel bars with specified size, both ends of the steel bars were drilled for further cable connection works.

b) Immersing Rebar in Solution

As this investigation was based on corrosion, before casting work all the steel bars were readied as fully rust free condition. To make steel bars rust free, steel bars before casting work were submerged in 10% Diammonium Hydrogen Sulphate solution for 24 hours. This solution reduced the bond strength among the steel bar surface and rusts which helped to remove rusts by rubbing with wire brush.

c) Cleaning Rebar's Using Wire Mesh

After keeping the steel bars immersed 24 hours in Diammonium Hydrogen Sulphate solution, steel bars were carefully rubbed with steel wire mesh to remove the rusts from steel surface. As any pre-existing rust in any rebar can significantly hamper the overall corrosion investigation process. To initiate the investigation all the steel bars were rubbed carefully to make them rust free and to bring them in a similar state.

d) Measuring Weight and Length of Bars

Then each steel bars weight and lengths were measured and were recorded. Weight of every steel bars were measured using digital weight machine. Length of steel bars were measured suing measuring tape very carefully. As after corrosion process, the generated rust becomes 5-8 times of its original volume and the formed rust could be removed by rubbing with wire mesh. Weight was measured so that the weight loss after corrosion process could be measured.

e) Connecting Electric Cable with Rebar

To make electrical investigation, connection establishment of electric cables with rebars were must. For making connection, each rebar's both ends were drilled and electric cables wires were placed inside each drill holes located at the both end of rebars. Then using Soldering Iron connections were made strong and durable enough so that the connections did not get damaged at the time of casting process.

f) Connection Testing Using Multi-Meter

After connecting the electric cables, it was necessary to ensure that every connection was working soundly. If the connections did not work properly, corrosion investigation could not be done. Due the loss of proper connection the whole corrosion investigation may be damaged. In this view every electric connections were checked using a Multi-meter device.

g) Adding Epoxy Gum to End of Rebar

After electrical connection test was done, epoxy gum was added at the end portions of the rebar to make the connections durable.

h) Final Washing of Steel Surface using Acetone

To remove any existing oil, Diammonium Hydrogen Sulphate solution or any other additional substances steel bars were finally washed by rubbing with a fresh piece of cloth with the presence of Acetone solution.

Different steps of reinforcement preparation before casting work have been illustrated in Fig. 3.4. below:

Cutting Steel Bars

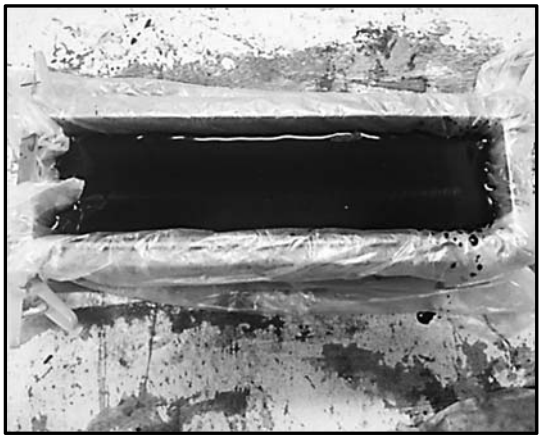

Steel Bars in Chemical Solution

Rubbing Steel Bars with Wire Mesh

Measuring Weight and Length

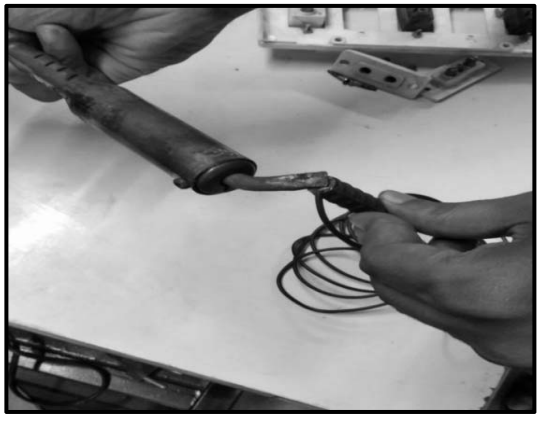

Connecting Electric Cables

Testing Connections Using Multi-meter

Fig. 3.4. Reinforcement Preparation Steps Prior to Casting

3.7 Coarse Aggregate Preparation

All three types coarse aggregates such as fresh brick aggregate (BA), stone aggregate (SA),and recycled brick aggregate (RBA) were broken into pieces manually in three particular sizes ranging from 25 mm to 19 mm, 19 mm to 9.5 mm and 9.5 mm to 4.75 mm. The maximum size of aggregates was 19 mm. After breaking into pieces, the aggregates were graded at 5% from 25 mm to 19 mm, 57.5% from 19 mm to 9.5 mm, and 37.5% from 9.5 mm to 4.75 mm as per ASTM C33-03. Before the preparation of concrete mixtures, the aggregates were kept in a submerged condition for 24 hours and were rubbed with clean cloth to eliminate excess water from the aggregate surface and to ensure the SSD condition of the aggregates.

3.8 Fine Aggregate Preparation

Two types of fine aggregates were used for this investigation. Natural river sand (NS) and recycled brick fine aggregate (RBFA). Prior to casting, both the fine aggregates were sieved through No. 4 (4.75 mm) sieve to separate any coarse aggregate from the mix and then washed to avoid mud and other organic materials. Sufficient water was mixed with sand several hours before casting and lump of sand was made in the palm of the hand. If the lump broke when the palm was stretched, the sand was considered to be in SSD condition. Once SSD fine aggregate was prepared, it was stored in airtight bags to avoid moisture loss.

3.9 Mold Preparation

Two shapes of specimens were casted for this investigation. 10 cm x 10 cm x 40 cm prism shaped specimen and 100 x200 mm shaped cylindrical specimen. Molds of both types of specimens were available at CEE Concrete Laboratory of Islamic University of Technology (IUT). Prior to casting, the molds were made air tight by adjusting the screws, and the inner surface was lubricated by using grease according to ASTM C 31 – 03.

3.10 Mixing of Fresh Concrete and Casting Procedure

For the casting of fresh concrete, mixture machine available in the Concrete Lab of Islamic University of Technology (IUT) was used. Trial mix was done in every case before the final mix. The mixing procedure followed in this study was quite different than the conventional mixing technique followed in construction sites in Bangladesh. The conventional technique is to put all the ingredients (cement, sand, coarse aggregate, water) simultaneously in the mixture. But in fact, it is not the best way to attain the desired strength of concrete. To ensure the quality of concrete the inner surface of the mixing machine was wiped with a moist piece of cloth, so that the surface wouldn't absorb the mixing water. Then half of the fine aggregate was poured into the machine and spread to give a notable bed like surface of the cement to put upon it. Cement was then placed on the sand bed. Rest of the fine aggregate was then poured on top of the cement. The sand and cement were then mixed for 30 seconds. Water was then poured into the sand-cement mixture carefully to avoid accidental spillage from the mixture machine. The machine was let to rotate and mix the cement-sand paste for one and a half minute more. The coarse aggregate was then introduced inside the mixing machine and the mixing was continued for further 3 minutes. The total mixing time was 5 minutes. After five minutes, the concrete mix was poured on a non-absorbent sheet to continue casting procedure simultaneously.

3.10.1 Casting of Cylindrical Specimen

The cylindrical samples were made according to ASTM C 31 – 03. First of all, the concrete sample was placed in the cylinder mold by moving the sampling tool used to pour concrete around the perimeter of the mold, to ensure even distribution and minimize segregation. Tamping rod of diameter 10 mm and length 300 mm was used to compact the concrete poured in cylinders in two layers. Each layer of concrete was tamped 25 times with the hemispherical end of the tamping rod. The bottom layer was tamped throughout its depth. The rodding was distributed uniformly over the cross section of the mold. For

upper layer, the tamping rod was allowed to penetrate through the layer being tamped and into the layer below by approximately 25 mm.

After rodding each layer, the outside of each mold was tapped lightly 10 to 15 times with a hammer, to close any holes and to release any large air bubbles that might have been trapped. After tapping, each layer of the concrete along the side of each mold was scaled with a steel scale. Under filled molds were adjusted with representative concrete during consolidation of the top layer. After consolidation, excess concrete from the surface was stroked off with a trowel.

3.10.2 Casting of Reinforced Prism Specimen

For each cases two reinforced prism specimens of 10 cm x 10 cm x 40 cm size were casted. For 16 cases total 32 prism specimens were made. In each prism specimen, two steel bars were placed, one as continuous bar to avoid collapse of the beams during cracking and one as segmented steel bar. The length of the continuous steel bar was 34 cm. The segmented steel bar were made by connecting three different segments with epoxy. The length of the end segments was 13.5 cm and the length of the middle segment was 5 cm. All the steel bars were pre-jointed with electric cables before casting concrete. While placing the steel bars color sequence for cables were maintained in as per below Figure 3.5 and Figure 3.6. Clear cover for steel bars were maintained 2 cm. Initially molds were filled up to 2 cm by fresh prepared concrete sample. Then using tamping rod of diameter 10 mm and length 300 mm, the concrete was evenly compacted. After that steel bars were placed ensuring 2 cm clear cover for all the steel bars. Then the steel bars were tied with very thin aluminum wire using a temporary support above the molds so that steel bars were not displaced for further tampering and hammering actions. Then the remaining part of the mold was filled with concrete samples and were tempered, hammered and scaled carefully. Finally the mold was hammered sufficiently to ensure there remains no void inside. Then after 5 min of casting work, thin aluminum cables were cut using cable cutter device and were ejected from specimens carefully.

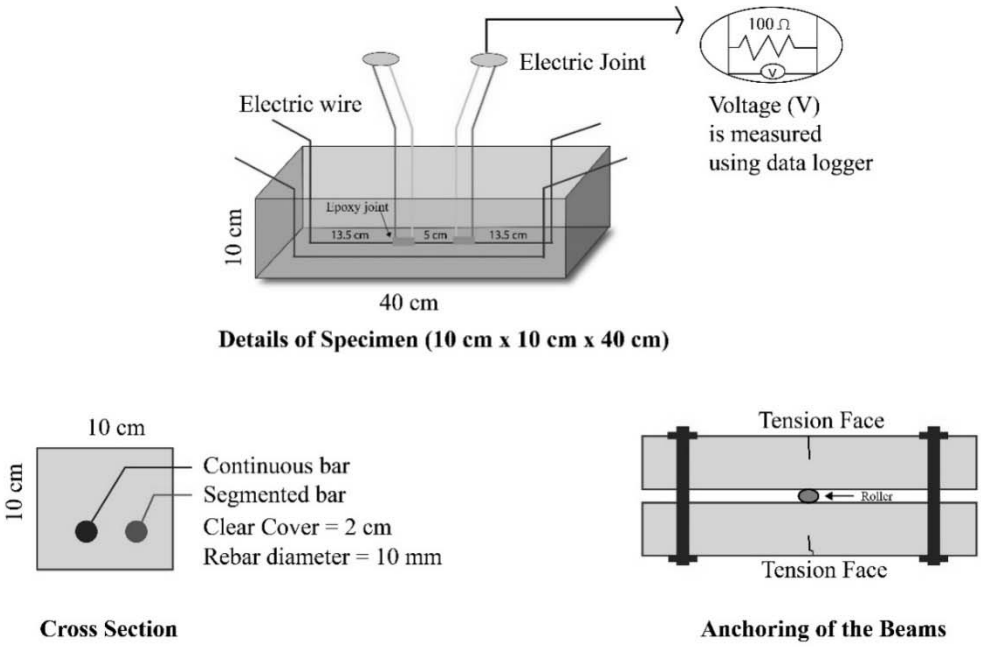

Fig. 3.5. Reinforcement Detailing and Cable Connection Details

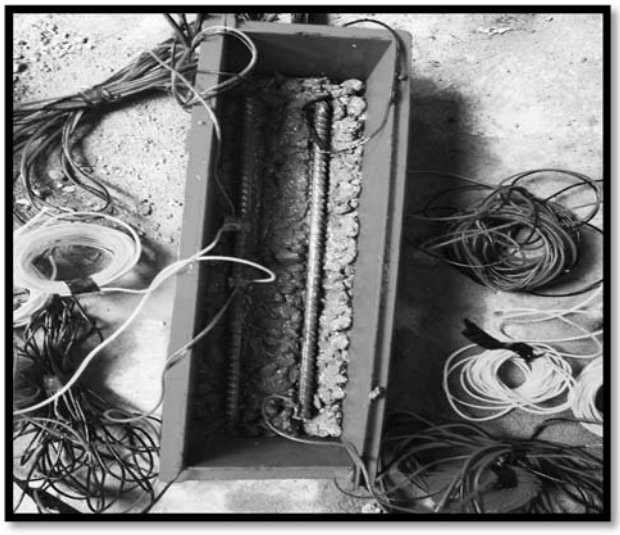

Fig. 3.6. Reinforcement Placement in Concrete

3.11 Curing of Specimens

The curing of specimens was done according to ASTM C192. To prevent the evaporation of water from the unhardened concrete, each specimen was immediately covered with wet burlap and a non-absorptive polythene sheet on top of the wet burlap. This initial curing of the specimens continued until the samples were demolded. After 24 hours of curing in the molds, the specimens were de-molded and cured under wet jute bags for 28 days.

3.12 Cracking of Specimens

After curing the reinforced prism specimens were kept in dry condition for several days. To fix the location of crack at the middle of prism specimen, a notch (3 mm wide and 5 mm depth) was made at the center of the bottom face of the specimens. Prism specimens were cracked by applying load at mid-span using a UTM (Universal Testing Machine).

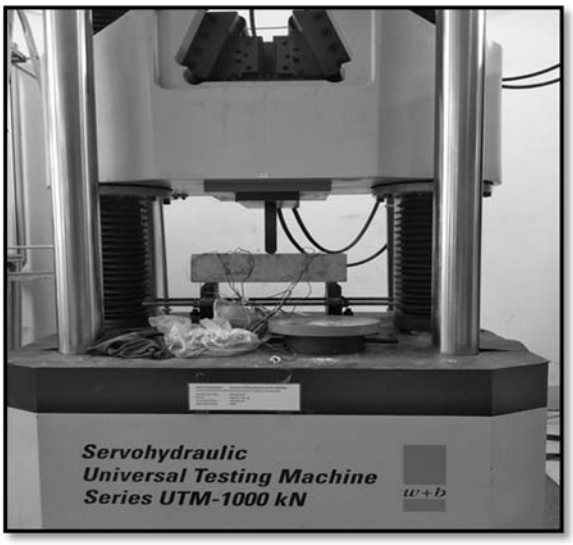

Fig. 3.7. Cracking of Specimens

3.13 Anchoring of Specimens

After cracking, the prism specimens were anchored in pair by back-to-back support with a roller at the middle as shown in Fig. 3.8. The crack width was very carefully controlled at 0.6 mm for all specimens while tightening the bolts of anchoring.

Fig. 3.8. Anchoring of Specimens

3.14 Exposure Condition

After anchoring, the specimens were kept at a seawater spray chamber where natural seawater was sprayed on the specimens once in a day for five minutes. The cylindrical specimens were submerged in 3% NaCl solution of temperature 40^{o}C. Natural sea water from Bay of Bengal was collected and used in slat spraying chamber. Mineral composition of natural sea water is shown on Table 3.9.

Table 3.9. Physical Properties and Mineral Composition of Sea Water

Component	pH	Na ppm	K ppm	Ca ppm	Mg ppm	Cl ppm	SO_4 ppm	CO_3 ppm
Amount	7.9	10752	390	416	1295	19345	2701	145

3.15 Testing

3.15.1 Compressive Strength

Compressive strength can be defined as the maximum stress a concrete specimen can withstand when loaded axially; it is one of the most important properties since concrete is subjected to compressive stresses in most structural applications. The compressive strength of concrete in this study was determined according to ASTM C 39. To determine the compressive strength the average compressive strength of two specimens having diameter 100 mm and height 200 mm was taken as per guideline of ASTM C 39 – 03. Since the specimen length to diameter ratio for cylinder samples was not less than 1.75, the compressive strength measured was not multiplied by any correction factor as specified by ASTM C 39 – 03.

3.15.2 Chloride Ingress in Concrete

After 28 days of curing, some cylindrical specimens were submerged in 3% NaCl solution of temperature 40^{o}C for 180 days for measuring chloride profiles in concrete at different ages of salt water exposure. For chloride measurements in concrete, a disc of height 100 mm was cut from the middle of the specimens. The discs were cut again to collect concrete samples from the different depths of specimens, such as 0~10, 10~20, 20~30, 30~40 and 40~50 mm from the surface to the center region of the specimens. Chloride profiles were measured after 120 days and 180 days of exposure in salt water.

The specimens were sliced as 10mm x10mm x 100mm strips as per Fig. 3.9 and made powder by a vibrating mill. The fine dust was separated after being sieved by #50 pan for A, B, C, D, E strips. For A strip 10 gm fine dust was mixed with 200 ml distilled water. And for the rest of the strips B, C, D & E 20 ml dust was mixed with 200 ml distilled water. For each case 5 liquid samples were collected. The fine dust was mixed with the distilled water and kept in 60^0C temperature for 30 minutes and after heating samples were kept in room temperature (24^0C) for next 24 hours. The fine powder of concrete contained chloride ions that ingressed from 3% sodium chloride (NaCl) water. Each separate liquid samples were titrated with silver nitrate ($AgNO_3$) solution and amount of chloride ion for each cases were measured.

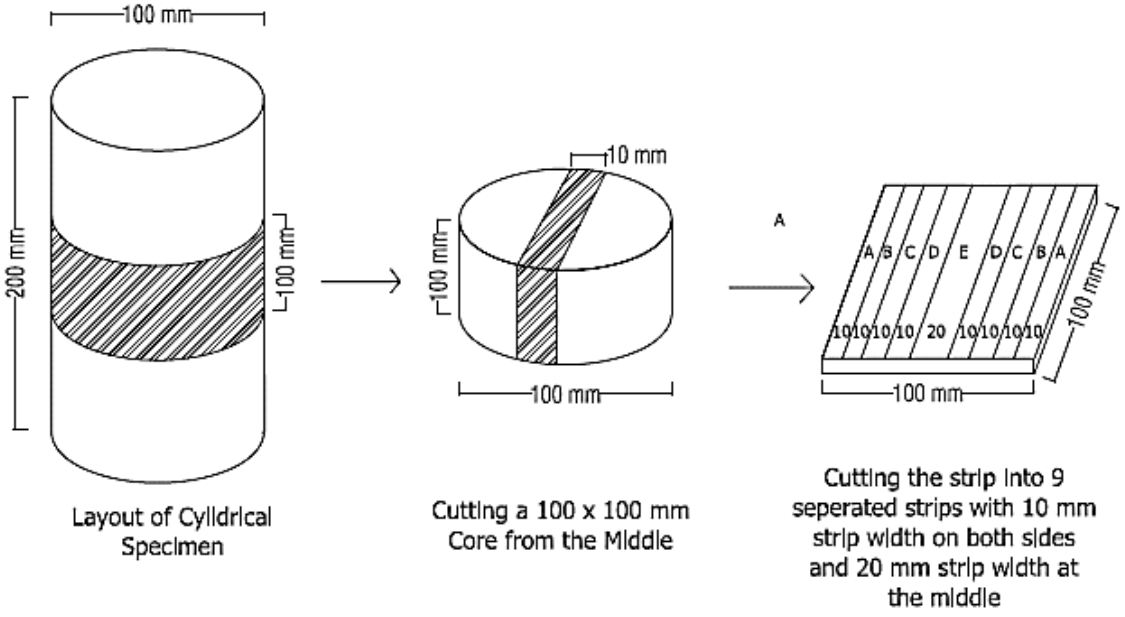

Fig. 3.9. Cutting Strips from Cylindrical Specimens for Titration

Chloride concentrations by mass percentage of cement used were determined by following Eq. (3.2) and Eq. (3.3) shown below:

$$s_1 = \frac{S2\ x\ V2}{V1} \tag{3.2}$$

Where, S_1 denotes chloride concentration, S_2 denotes silver nitrate concentration, V_1 and V_2 denotes volume of filtered water used for titration and volume of silver nitrate used respectively.

$$Cl_{con} = \frac{VMS_1Y_{con}}{1000Xc} \tag{3.3}$$

Where, Cl_{con} means chloride concentration in mass percentage of cement, V denotes volume of sample used, M denotes atomic weight of chloride (35.45), S_1 denotes chloride concentration, Y_{con} denotes unit weight of concrete, X denotes mass of sample powder used, C denotes cement content in 1 m^3 of concrete.

Chloride concentration around steel bars at cracked and un-cracked regions were measured after electrochemical investigations. For this concrete samples were collected around the steel bars both for cracked region and un-cracked regions. Then chloride concentrations were measured as per JCI SC4.

3.15.3 Macro-Cell Corrosion

To measure macro-cell corrosion, a data logger was used. At each joint of electrical connection, a 100 Ω resistance was placed to measure voltage drop due to the movement of electrons from anode (cracked segment) to cathode (un-cracked segment). As cracked

was made at the middle of the specimens, therefore, the middle segment of steel acted as anode and the others two segments (end segments) as cathodes. The voltage drops were continuously recorded for 30 days using a data logger at a pre-fixed interval of time as summarized in Table 3.10. A photograph showing the setup of data logger is shown in Fig. 3.10. The following equation (Ohm's Law) was used to calculate the current flow from the measured voltage drop through a fixed resistance of 100 Ω:

$$I = \frac{V}{R} \tag{3.4}$$

Where R is resistance (100 Ω), and V is potential (in *Volt*) and I is current (in *ampere)*. The following equation was used to calculate macro-cell corrosion current density:

$$I_{mac} = \frac{I}{A} \times 10^6 \tag{3.5}$$

Where, A is the surface area of the steel segment in cm^2, I is the macro-cell current in A, and I_{mac} is the macro-cell corrosion current density in $\mu A/cm^2$. It is worth noting that to calibrate the voltage measurement system, known currents of 1, 2 and 3 μA were passed through 100 Ω resistance and the voltage drops against these currents were 99, 198 and 298 mV, respectively. The results indicate that the experimental setup can measure current flow between the steel bars accurately.

The depth of corrosion over the steel bars was calculated by using the following equation:

$$D = 0.0116 \times I_{mac} \times t \quad (3.6)$$

$where\ D$ is the depth of corrosion in mm, I_{mac} is the macro-cell corrosion current density in $\mu A/cm^2$, and t is time in year.

Table 3.10. Time Schedule of Voltage Drop Measurement by Data Logger

Total Period	Interval of Measurement
30 days	Measure immediately before spray, after spray first 5 minutes at every 1 sec interval, next 30 minutes at every 5 minutes, next 1 hour at every 10 minutes, next 4 hours at every 30 minutes and then at every 1 hours or immediately before spray.

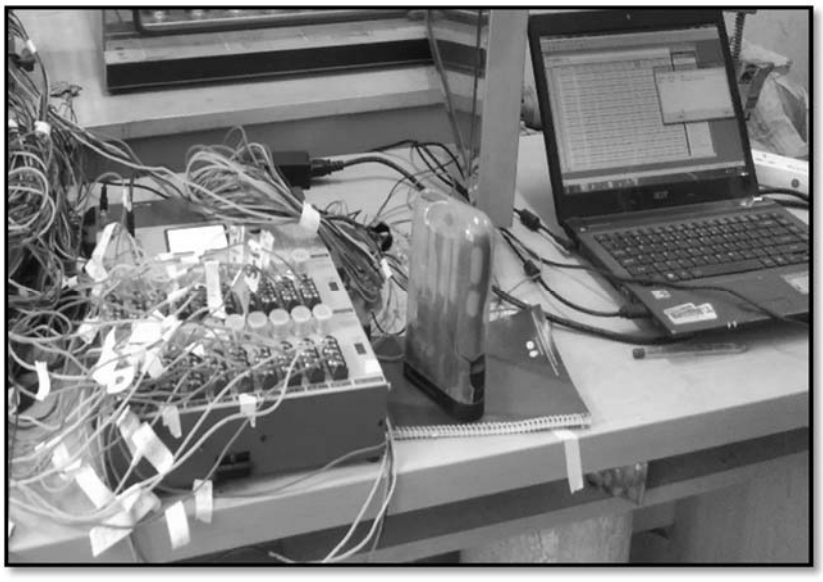

Fig. 3.10. Macro-cell Corrosion Measurement Using Data Logger Device

3.15.4 Micro-Cell Corrosion

Micro-cell corrosion was measured using a device named Corro-Map. It was measured by connecting a cable both from the middle segmented steel bar of 5 cm and continuous steel bar of 34 cm with Corro-Map device. Macro-cell corrosion measurements were taken before exposure period and after completion of salt water spraying exposure period of 30 days. As per Micro-Cell corrosion values, corrosion level can be categorized as per Table 4.1 below (Andrade and Alanso, 2001

Table 3.11. Levels of Micro-Cell Corrosion

Corrosion Rate (μA/cm²)	Corrosion Level
< 0.1	Negligible
0.1-0.5	Low
0.5-1.0	Moderate
>1.0	High

3.15.5 Half-Cell Potential

Half-cell potential was measured using a *$Cu/CuSO_4$* half-cell. The half-cell potentials over the segmented steel bars were measured after completion of continuous measurement of macro-cell corrosion current for a period of 30 days. It was done to avoid interference in the flow of macro-cell corrosion current. During measurement of potential of a particular segment of steel, the segment was isolated electrically from others. Corrosion probability for different half-cell potential *($Cu/CuSO_4$)* values were determined

as per ASTM C876 as explained in Table 3.12. Half-cell potential measurement using Cu/CuSO4 solution is shown on Fig. 3.11.

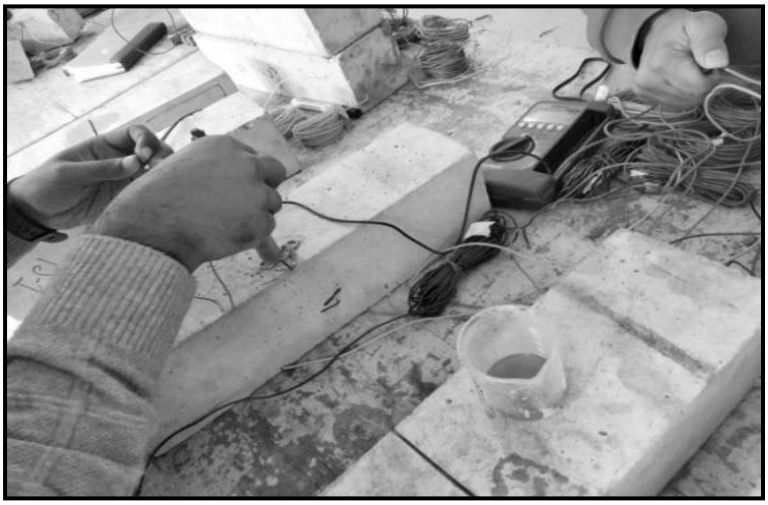

Fig. 3.11. Half-Cell Potential Measurement Using $Cu/CuSO_4$ Solution

Table 3.12. Half-Cell Potential and Probability of Corrosion (ASTM C876)

Half-Cell Potential Reading (mV)	Corrosion Probability (%)
Greater than -200 mV	90% probability of no corrosion
Between -200 mV to -350 mV	Intermediate corrosion risk (uncertain)
Less than -350 mV	90% probability of corrosion

3.15.6 Concrete Resistance

Concrete resistance was measured using a device named Corro-Map. It was measured by connecting a cable from the segmented steel bar at the cracked region with Corro-Map device after completion of salt water spraying exposure period of 30 days.

Fig. 3.12. Concrete Resistance Measurement

3.15.7 Visual Observation, Corroded Area and Pit Depth Calculation

After completion of macro-cell corrosion current measurement, the prism specimens were broken open and steel bars located at both cracked and un-cracked regions of the specimens were taken out for visual observation and measurement of corrosion area and the depth of corrosion pits. To measure corrosion area over steel bars, the corrosion area on the steel bars was traced on a transparent paper. The depths of corrosion were measured by inserting nails into the pits. Corroded area measurement is shown on Fig. 3.13.

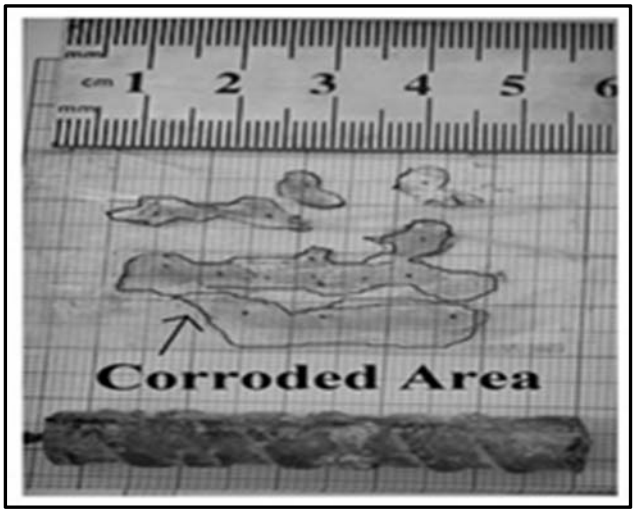

Fig. 3.13. Corroded Area Measurement for Steel Bars

.

CHAPTER 4: RESULTS AND DISCUSSIONS

4.1 General

In this chapter, the results obtained throughout the investigation are summarized and discussed. The 28 days compressive strength for all the cases have been exhibited. Chloride ingress amount for different types of aggregates, for different types of cement contents and w/c ratios have been described in this chapter with graphical representations. Along with chloride ingress, progress of macro-cell corrosion have been described in this chapter. Half-cell potential and concrete resistance values at the cracked and un-cracked regions have been shown in this chapter. Comparative chloride ingress amount at both cracked and un-cracked regions for the prism shaped specimens have been analyzed graphically in this chapter. Physical observations for rebars, corroded area measurement values with images, pit depths, rebar surface condition have also been exhibited in this chapter.

4.2 Compressive Strength

4.2.1 Effects of Aggregates on Compressive Strength

Concrete made with different types of aggregates results in different types of compressive strengths. For measurement of compressive strength, 100 x 200 mm cylindrical shaped concrete cylinders were prepared. For each case, 2 cylinders were made for measuring compressive strength. 28 days compressive strengths were measured in the CEE Concrete Laboratory of Islamic University of Technology. The results of 28 days compressive strengths are shown below graphically-

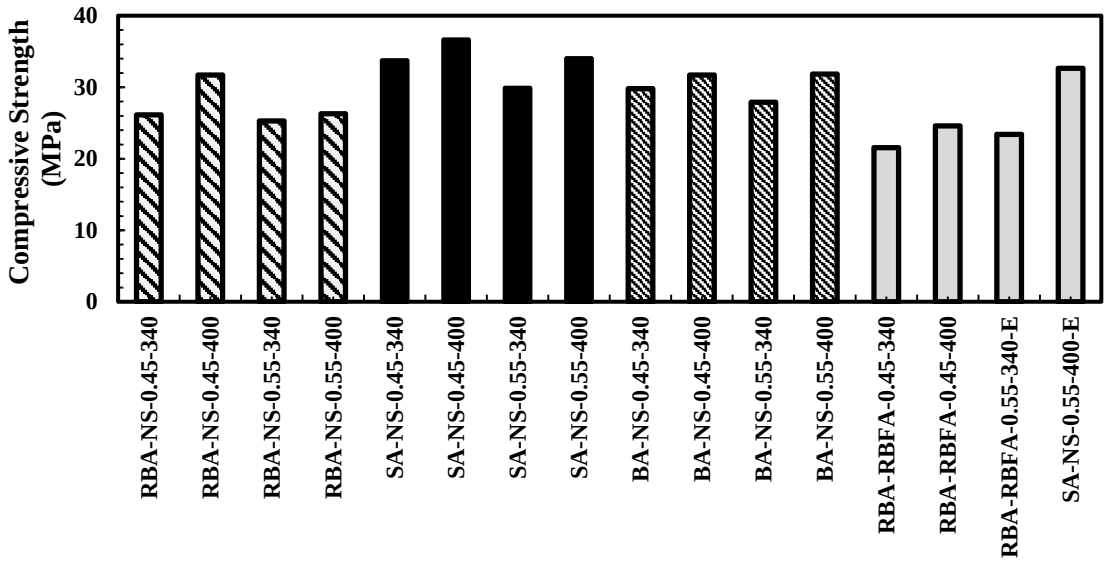

Fig. 4.1. 28-Days Compressive Strength for Different Aggregates

Beshr et al. (2003) concluded that in a high strength concrete, i.e. concrete prepared using a low w/c ratio and high cement content, the compressive strength is dependent on the quality of aggregate. As per the results shown on Figure 4.1 it is clear that concrete made with stone aggregate as coarse aggregate with combination of coarse sand as fine aggregate exhibits maximum level of compressive strength. On the contrary, concrete made with recycled brick aggregate exhibits least amount of compressive strength. As fine aggregate coarse sand (NS) contributes to higher compressive strength than using recycled brick fine aggregate (RBFA) as fine aggregate. Similar result was also observed in some previous studies on recycling of demolished brick aggregate concrete. (Mohammed et al., 2015).

As per compressive strength higher to lower, types of coarse aggregate used in concrete can be sequenced as SA> BA> RBA.

4.2.2 Effects of Cement Content on Compressive Strength

The effect of different cement content on 28 days compressive strength of concrete is shown in Figure 4.2. Two different types of cement contents of 340 and 400 kg/m^3 were used in this study. Based on Figure 4.2, it can be summarized that, the compressive strength increases with an increase of cement content for both w/c 0.45 and 0.50 separately.

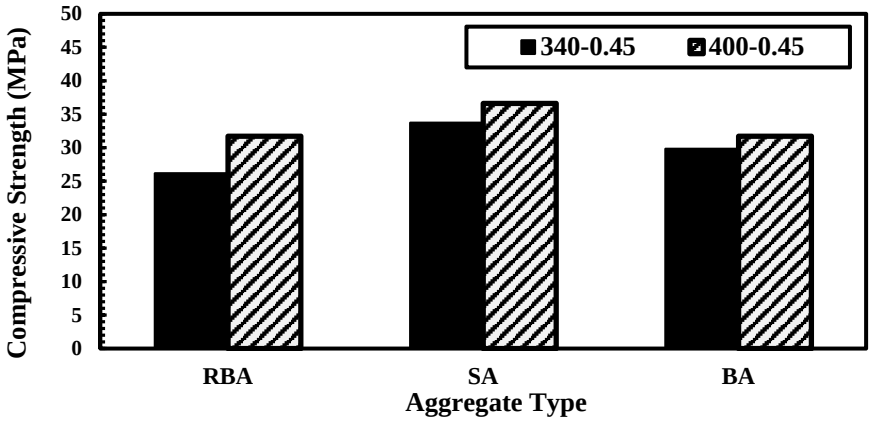

(a) For w/c ratio = 0.45

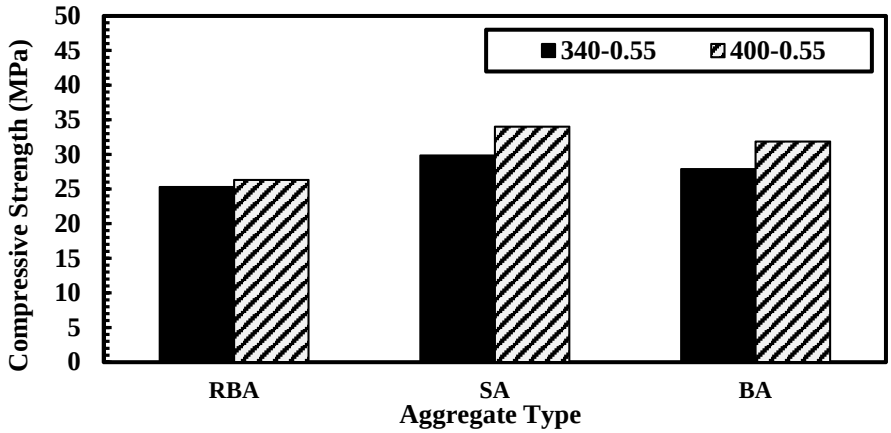

(b) For w/c ratio = 0.50

Fig. 4.2. Compressive Strength: Variation of Cement Content

4.2.3 Effects of W/C Ratio on Compressive Strength

The strength of concrete increases with the decrease of w/c ratios (Demirboga and Gul, 2006). From the Fig. 4.3 it was observed that with the increase of w/c ratio the compressive strength got decreased. With the increase of water content, cement content gets decreased which leads to a large air-filled void in the concrete making it porous. This results in a decrease in materials, reduced number of bonds between paste and aggregates, and they act as stress concentrations leading to a reduction in strength.

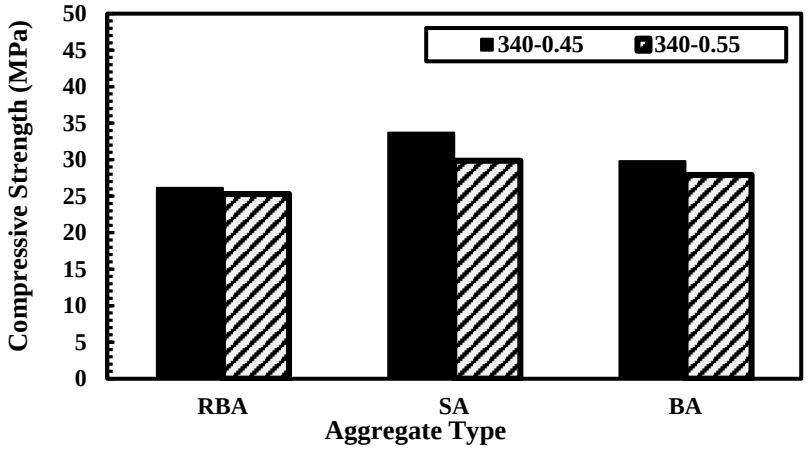

a) For Cement Content= 340 kg/m^3

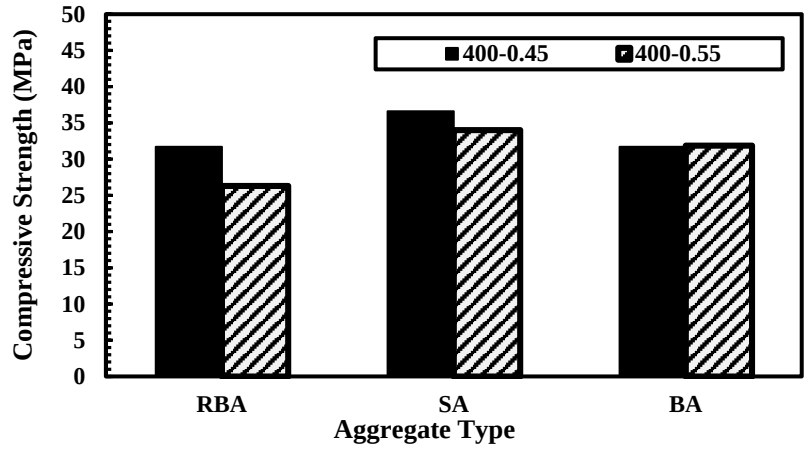

b) For Cement Content= 400 kg/m^3

Fig. 4.3. Compressive Strength: Variation of W/C

4.3 Chloride Profiles for Cylindrical Specimens at 120 and 180 Days

Concrete cylinders of 100 x 200 mm size were prepared for the testing of accelerated chloride ingress test. The cylinders were kept at saline water at 40^0C temperature with 3% concentration of NaCl. At 120 and 180 days the cylinders were cut into pieces to measure the amount of chloride concentrations. As per the measured values of chloride concentrations, chloride ingress mechanism variation for different types of aggregates, different w/c ratios and cement contents were established.

For different micro structures, different aggregates represented different rates of chloride ingress. The chloride profiles for different aggregates for 120 days are shown graphically in Figure 4.4.

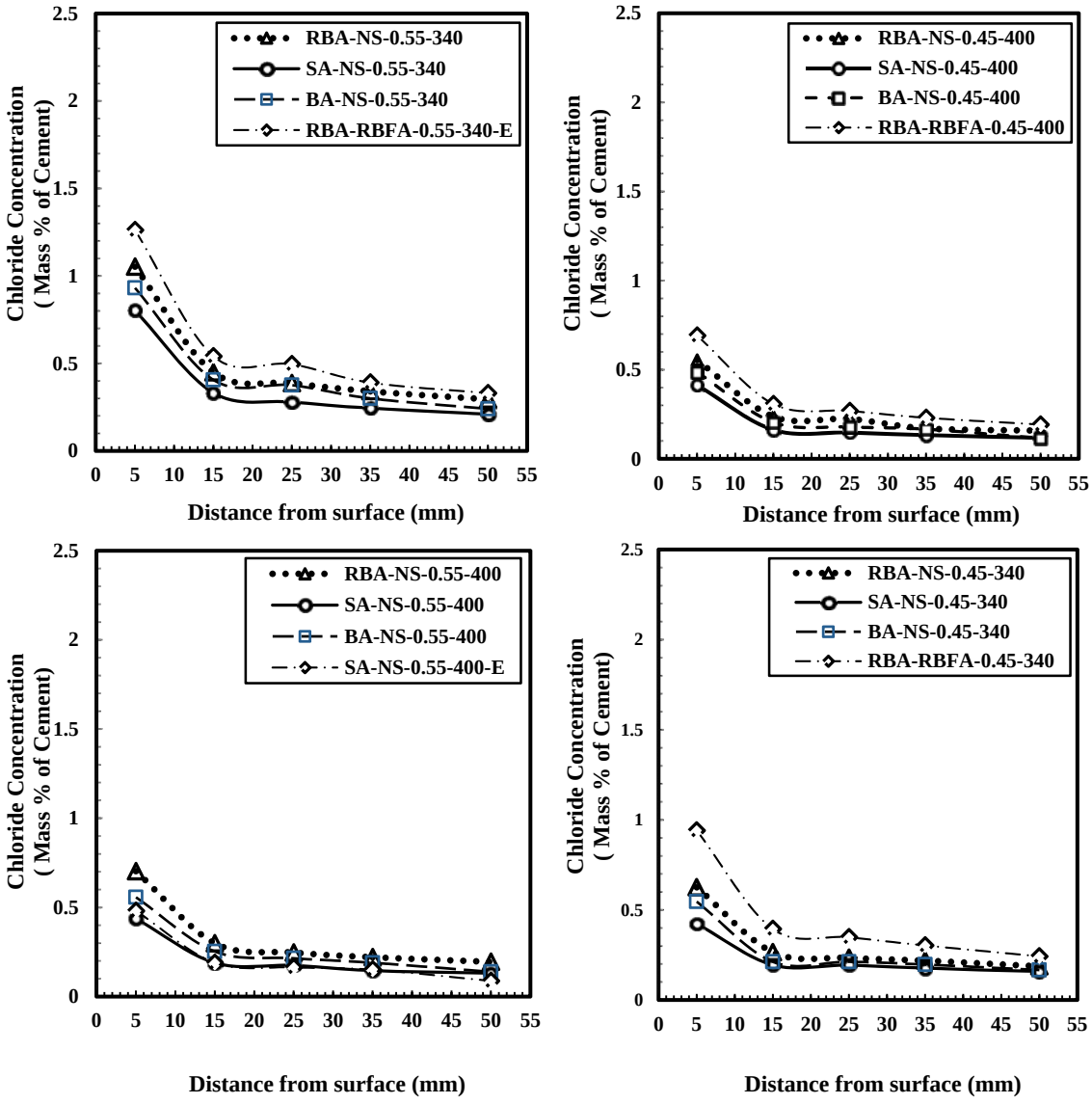

Fig. 4.4. Chloride Profiles after 120 Days of Exposure in Salt Water

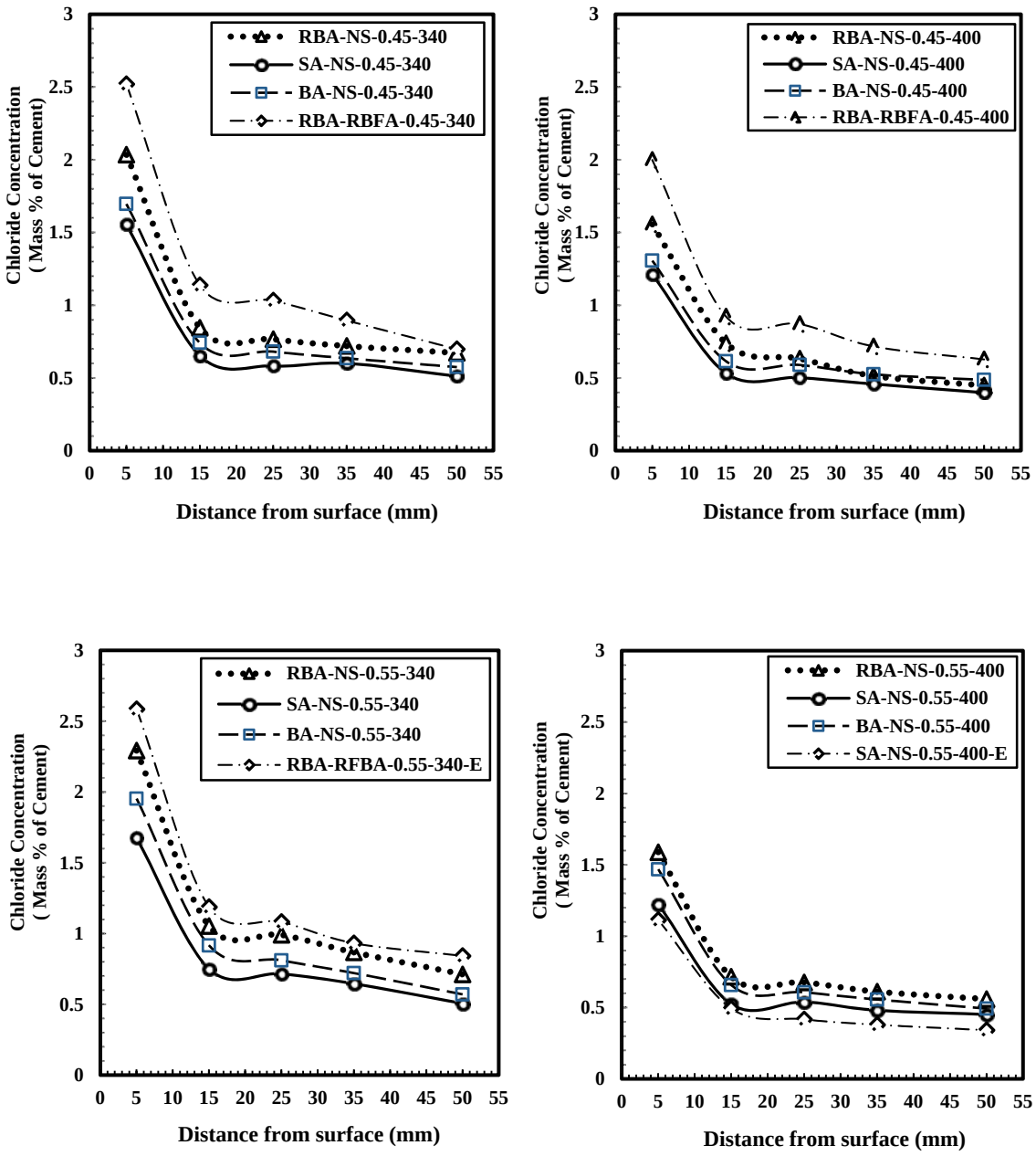

Fig. 4.5. Chloride Profiles after 180 Days of Exposure in Salt Water

The chloride concentrations at 50 mm depth from surface of cylindrical specimens for all the cases after 120 days and 180 days are shown respectively on Fig. 4.6. and Fig. 4.7.

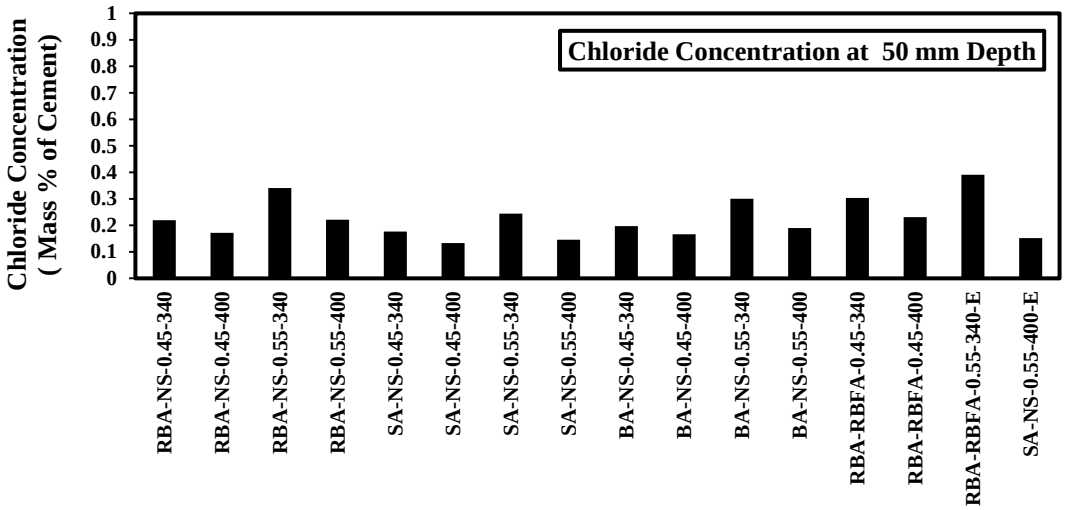

Fig. 4.6 Chloride Concentrations at 50 mm Depth from Surface at 120 Days

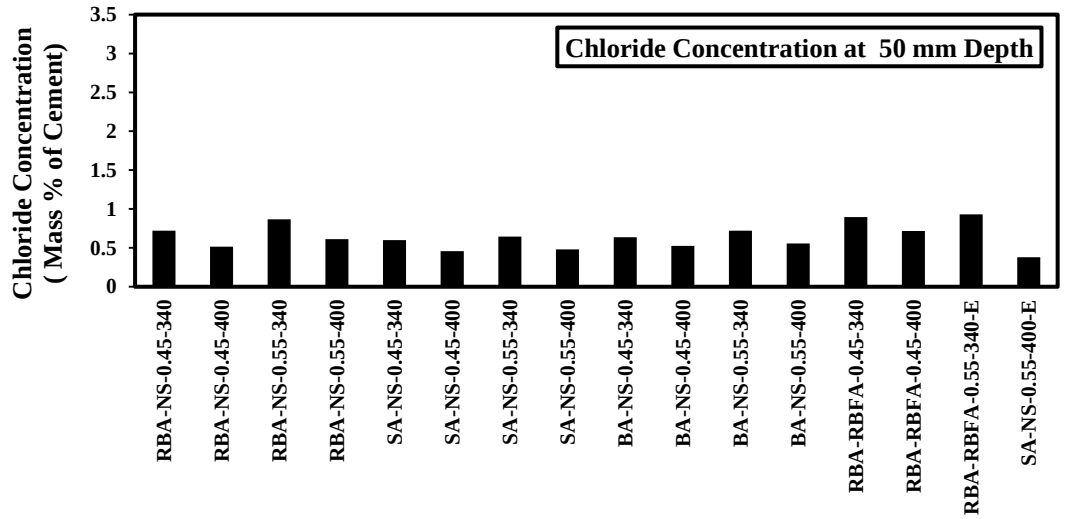

Fig. 4.7. Chloride Concentration at 50 mm Depth from Surface at 180 Days

From Fig. 4.4, Fig. 4.5, Fig. 4.6 and Fig. 4.7 chloride ingress rate with respect to type of aggregates can be sequenced from higher to lower order as RBA> BA > SA. This variation is due to the ITZ (Interfacial Transition Zone) variability of different types of aggregates. For having more water absorption rate and porous ITZ recycled brick aggregate (RBA) showed highest level of chloride ingress rate. On the contrary concrete made with stone aggregate represented comparatively lower porosity as well as less water absorption tendency comparing with RBA and BA. For having stronger interfacial transition zone, SA exhibited highest resistivity against chloride ingress. Again concrete made with recycled brick fine aggregate (RBFA) showed significantly higher level of chloride ingress rate comparing with concrete made with natural river sand (NS). Concrete made with recycled brick aggregate both as coarse and fine aggregate with lower cement content and higher w/c ratio had shown maximum amount of chloride ingress rate.

4.4 Chloride Concentration at Cracked and Un-Cracked Regions of Prism Specimens

Chloride concentrations around the steel bars in concrete at the cracked and un-cracked regions of the prism specimens are shown in Fig. 4.8. Higher amount of chloride was found over the steel bar at the cracked region compared to the steel bar at the un-cracked region. For the un-cracked regions chloride concentration was less than the threshold limit of chloride against corrosion of steel in concrete (0.4% mass of cement mass). On the other hand, at the cracked region, the chloride level around the steel bars exceeds chloride threshold limit against corrosion of steel in concrete. Due to the difference in chloride levels, it is understood that macro-cell corrosion cell over the steel bar will be formed with anode at the cracked region and cathode at the un-cracked region. More chloride is found around the steel bars for the cases made with RBA and BA compared to SA. Therefore, macro-cell corrosion activities over the steel bars for concrete made with RBA and BA will be higher than the concrete made with SA.

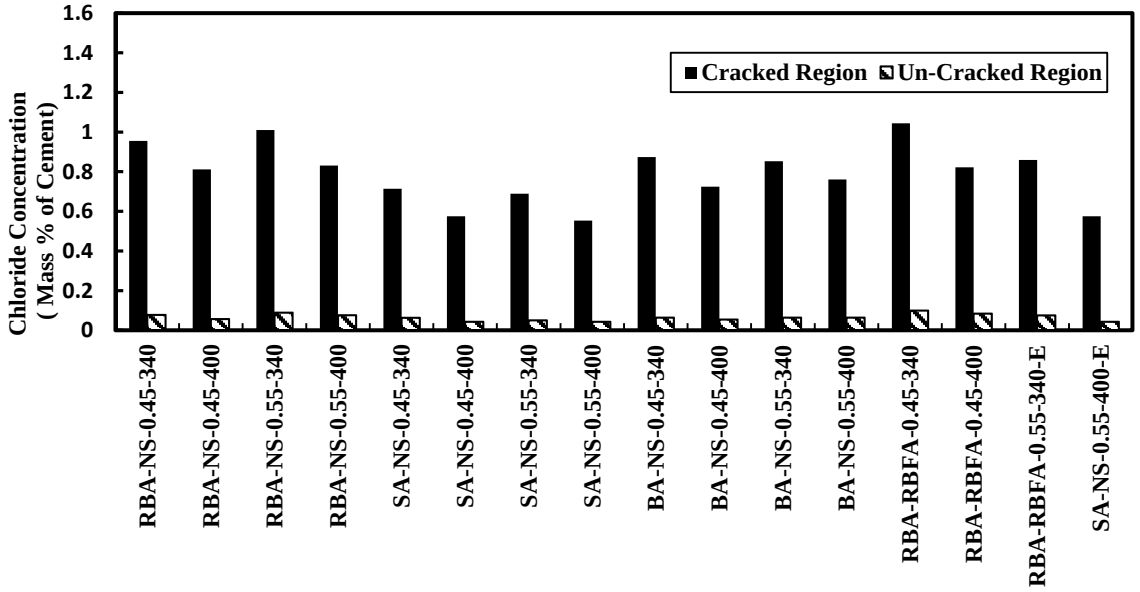

Fig. 4.8. Chloride Concentrations around Steel Bars at Cracked and Un-cracked Region

4.5 Macro-Cell Corrosion

For all the 16 cases, macro-cell corrosion was measured using Data Logger machine. The comparative effect of aggregates, w/c ratio and cement content on macro-cell corrosion are shown on Fig. 4.9, Fig. 4.10 and Fig. 4.11 accordingly.

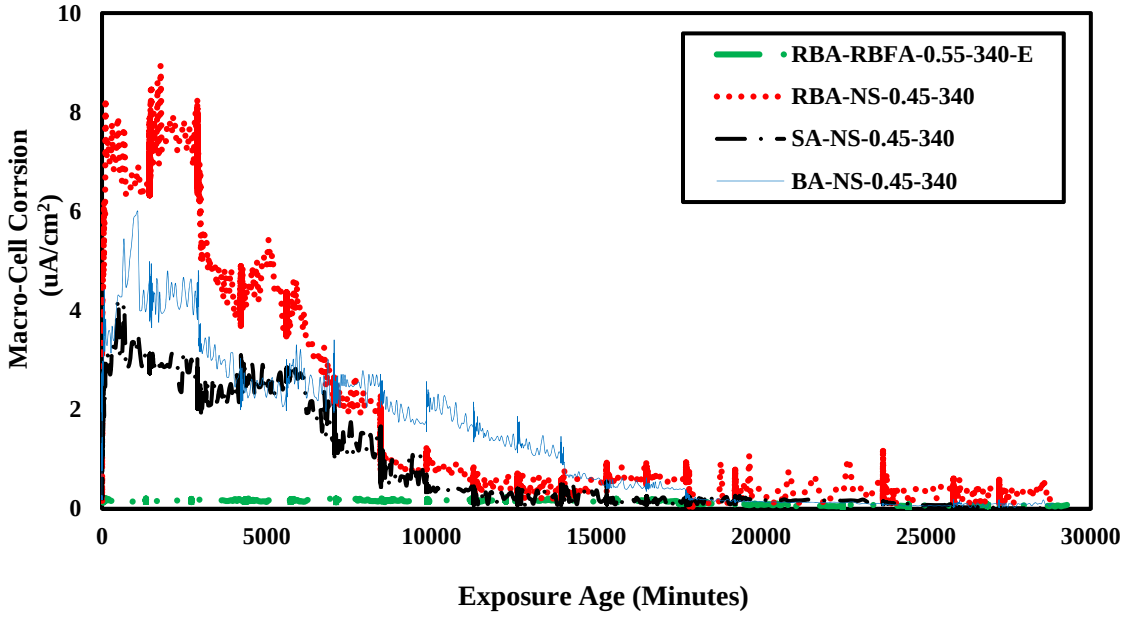

Fig 4.9. Effect of Type of Aggregates and Epoxy Coated Bar on Macro-Cell Corrosion

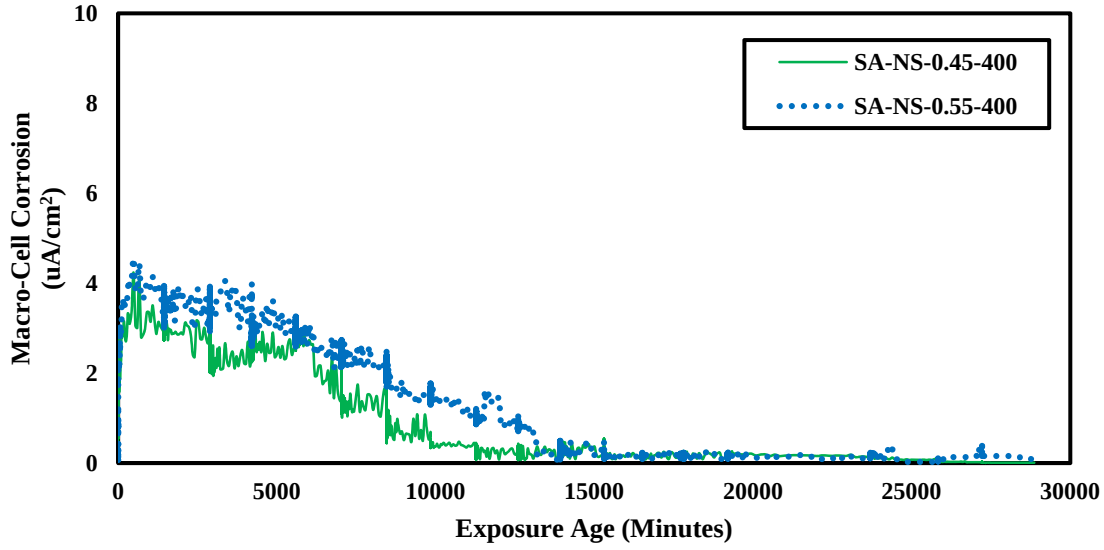

Fig 4.10. Effect of W/C on Macro-Cell Corrosion

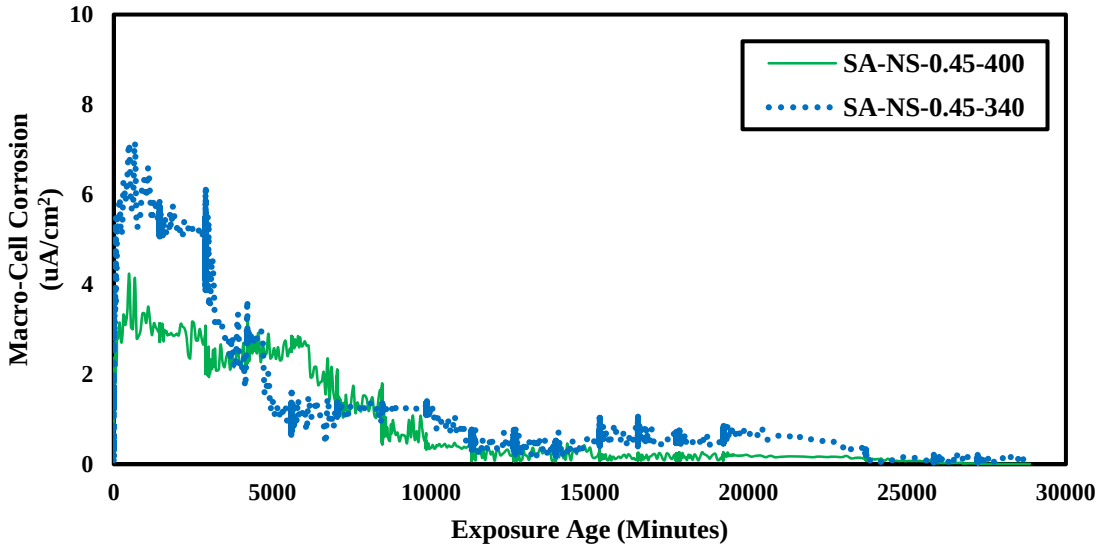

Fig 4.11. Effect of Cement Content on Macro-Cell Corrosion

It is seen that due to the spray of seawater over the specimens, the rate of macro-cell corrosion is increased immediately but reduced over time till the next seawater spray. However, the peak is reduced gradually with time. The level of macro-cell corrosion current density is increased at the early age of exposure but later it is reduced gradually. The reduction of macro-cell corrosion current density over steel bars at the cracked regions of concrete is explained in a previous investigation on macro-cell corrosion (Mohammed, et al., 2011). After detailed investigation by using Scanning Electron Microscope, deposits of ettringite, $CaCO_3$, and $Mg(OH)_2$ were found at the cracked openings as well as over the debonded steel at the cracked regions. Even the rusts over the steel bars at the cracked regions were covered by these deposits due to the spray of seawater (Mohammed, et al.,

2011). The reduction of macro-cell corrosion of this study is well matched with the previous investigation. As per Fig. 4.9 it is seen that higher level of macro-cell corrosion current density is observed for concrete made with RBA compared to the BA and SA. The rate of macro-cell corrosion current density over the steel bars with respect to the types of aggregate can be ordered as RBA>BA>SA. The porous nature of RBA and BA are responsible for higher level of macro-cell corrosion current density over the steel bars. However, to use RBA and BA for construction works we need to enhance the microstructure of mortar portion of concrete by reducing w/c and increasing cement content which will eventually reduce the permeability of concrete as per Fig. 4.10 and Fig. 4.11. A very low level of macro-cell corrosion is found for epoxy coated bars compared to the bared steel irrespective of types of aggregate. Similar effectiveness of epoxy coated bar was previously reported in many studies (Lopaz, et al., 2012, Kobayashi, et al., 1984, and Pour-Ali, et al., 2015).

For further comparison of corrosion at the cracked region of the specimens, the areas under the macro-cell corrosion and time curves were calculated. The data can be used to compare macro-cell corrosion activity of steel bars in concrete made with different aggregates. The results are summarized in Table 4.1. The depths of corrosion over steel bars were also calculated using Eq. 3.4 and summarized in Table 4.1. The rankings based on the corrosion activity over the steel bars (more corrosion to least corrosion) were evaluated and the results are summarized in Table 4.1. More corrosion activity is found over the steel bars in concrete made with RBA. The porous nature of BA and RBA causes to enhance corrosion activity over the steel bars in concrete. The results matched well with

the data related to chloride ingress in concrete as discussed earlier. The cases made with higher w/c with lower cement content show higher level of corrosion due to the porous microstructure of concrete. Similar results were also reported in other studies (Nanayakakkara, et al, 2009).

Table 4.1 Area under Corrosion-Time Curve, Depth of Corrosion, and Ranking

Case	Case Identification	Area Under Corrosion-Time Graphs ($\frac{\mu A}{cm^2}.Year$)	Depth of Corrosion (mm)	Ranking*
C13	RBA-RBFA-0.45-340	0.184	0.00214	1
C14	RBA-RBFA-0.45-400	0.143	0.00166	2
C11	BA-NS-0.55-340	0.133	0.00155	3
C12	BA-NS-0.55-400	0.120	0.00140	4
C3	RBA-NS-0.55-340	0.105	0.00123	5
C1	RBA-NS-0.45-340	0.095	0.00111	6
C4	RBA-NS-0.55-400	0.093	0.00108	7
C9	BA-NS-0.45-340	0.074	0.00087	8
C2	RBA-NS-0.45-400	0.071	0.00083	9
C5	SA-NS-0.45-340	0.068	0.00079	10
C8	SA-NS-0.55-400	0.066	0.00077	11
C10	BA-NS-0.45-400	0.062	0.00073	12
C6	SA-NS-0.45-400	0.046	0.00054	13
C7	SA-NS-0.55-340	0.044	0.00051	14
C15	RBA-RBFA-0.55-340-E	0.008	0.00010	15
C16	SA-NS-0.55-400-E	0.007	0.00008	16

*descending order of corrosion activity.

4.6 Micro-Cell Corrosion

Macro-cell corrosion values were measured both for 5 cm segmented steel bar located at the cracked region and for the 34 cm continuous steel bar located at the un-cracked region. Macro-cell corrosion values before exposure and after exposure are shown in Table 4.1 and Table 4.2 accordingly.

Table 4.2. Micro-Cell Corrosion before Exposure

Case	Case Denotation	Segmented Bar ($\mu A/cm^2$)	Continuous Bar ($\mu A/cm^2$)
1	RBA-NS-340-0.45	1.3	0.6
2	RBA-NS-400-0.45	0.5	1.5
3	RBA-NS-340-0.55	1.3	2
4	RBA-NS-400-0.55	1.5	1.2
5	SA-NS-340-0.45	<.5	<.5
6	SA-NS-400-0.45	1.8	0.5
7	SA-NS-340-0.55	0.6	1.4
8	SA-NS-400-0.55	<.5	1.2
9	BA-NS-340-0.45	1.4	0.5
10	BA-NS-400-0.45	0.6	<.5
11	BA-NS-340-0.55	<.5	1.7
12	BA-NS-400-0.55	0.6	0.5
13	RBA-RBFA-340-0.45	1.4	0.8
14	RBA-RBFA-400-0.45	<.5	1.2
15	RBA-RBFA-340-0.55-E	1.2	<.5
16	SA-NS-400-0.55-E	1.3	1.4

Table 4.3. Micro-Cell Corrosion after Exposure

Case	Case Denotation	Segmented Bar μA/cm²	Continuous Bar μA/cm²
1	RBA-NS-340-0.45	0.5	0.8
2	RBA-NS-400-0.45	0.5	1.4
3	RBA-NS-340-0.55	1.4	1.9
4	RBA-NS-400-0.55	1.6	1.4
5	SA-NS-340-0.45	0.8	0.8
6	SA-NS-400-0.45	1.5	1.2
7	SA-NS-340-0.55	<.5	1.1
8	SA-NS-400-0.55	<.5	1.4
9	BA-NS-340-0.45	1.6	<.5
10	BA-NS-400-0.45	0.5	0.5
11	BA-NS-340-0.55	<.5	1.7
12	BA-NS-400-0.55	<.5	1.6
13	RBA-RBFA-340-0.45	1.8	1.4
14	RBA-RBFA-400-0.45	1.1	1.6
15	RBA-RBFA-340-0.55-E	1.4	<.5
16	SA-NS-400-0.55-E	0.5	1.2

Unfortunately, from Table 4.2 and Table 4.3, it was seen that the different values of Micro-cell corrosion were not acceptable. Even before exposure of the specimens, there were found extreme level of corrosion (more than 1 μA/cm²) which did not seem to be acceptable. There were not seen any significant difference of macro-cell corrosion values both for segmented and continuous steel bars before or after exposure. Faulty data were shown by the Corro-Map device due to internal malfunction which could not be solved. That's why the Macro-cell corrosion values were not considered to draw any conclusion.

4.7 Half Cell Potential

Half-cell potentials over the steel bars at cracked and un-cracked regions after 30 days of seawater exposure are shown in Fig. 4.12. It is observed that half-cell potential values over the steel bars at the cracked regions were more negative than -350 mV which indicated 90% probability of active corrosion as per ASTM C876 as summarized in Table 3.12. On the contrary, half-cell potential values at the un-cracked regions of the specimens were found to be more positive than -200 mV which indicated only 10% probability of corrosion. The half-cell potentials at the cracked and un-cracked regions of steel bars indicate that macro-cell corrosion cell will form with anode at the steel segment and cathodes at the two ends of the steel segments. The results matched with the macro-cell corrosion current density data as explained earlier and similar observations were found from previous corrosion investigation by Mohammed, et al., 2011. Epoxy coated bars showed no corrosion irrespective of cracked and un-cracked regions.

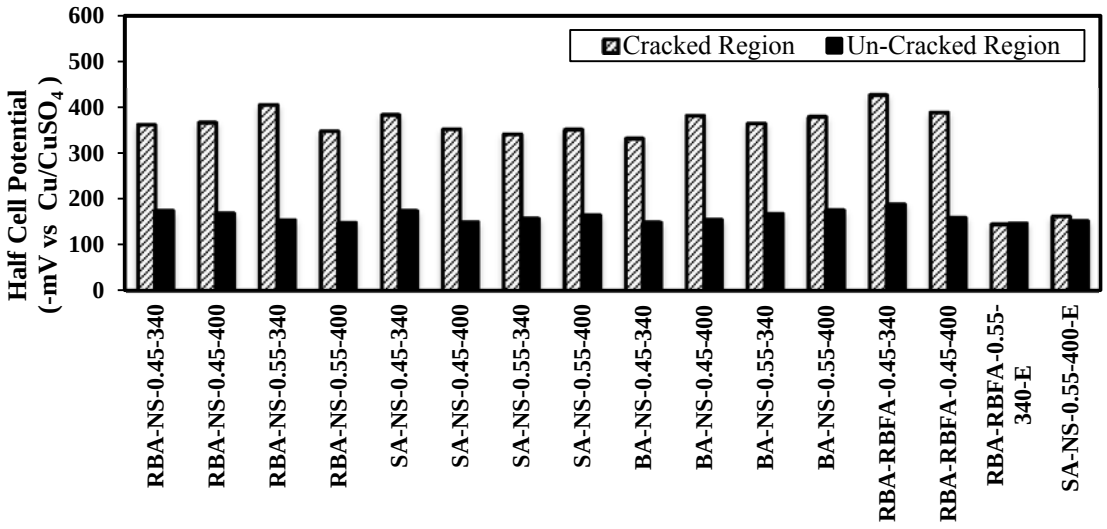

Fig. 4.12. Half-cell Potential Values at Cracked and Un-Cracked Region

4.8 Concrete Resistance

Electrical resistivity of concrete is highly dependent on the microstructural properties of the concrete (Layssi et al., 2015). Lower permeability leads to higher concrete resistance values. The data related to concrete resistance at cracked region after the end of seawater exposure are shown in Fig. 4.13. Relatively less concrete resistance is found for the cases made with RBA and BA compared to SA. With respect to the type of aggregate, concrete resistance can be ordered as SA>BA>RBA. The more chloride ingress in concrete as well as more macro-cell corrosion activity of steel bars in concrete made with RBA and BA can be explained due to the lower concrete resistance. The cases with higher W/C also show less concrete resistance.

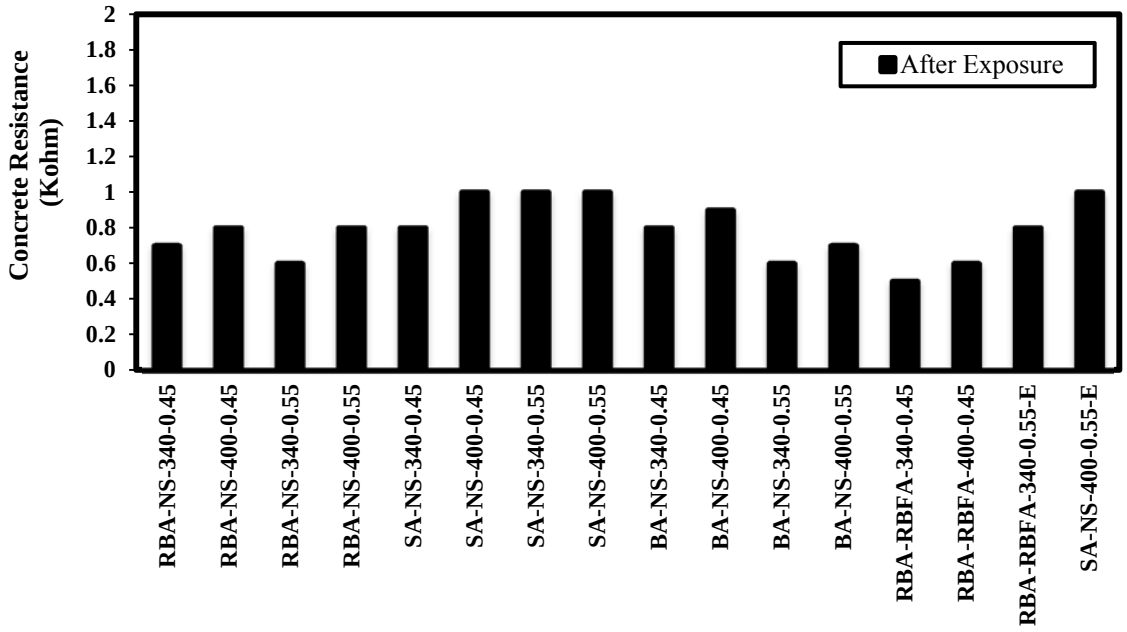

Fig. 4.13. Concrete Resistance Values

4.9 Corroded Area and Pit Depth Observation

Corroded areas and pit depths over the steel bars were measured after electrochemical investigations. The results are summarized in Table 4.4 and Table 4.5. Higher percentages of corroded area were observed for the segmented steel bars at the cracked region compared to the un-cracked regions as expected from the electro-chemical data.

Table 4.4. Corroded Area and Pit Depth at Cracked Region

Case	Short Description	Corroded Area (cm^2)	Percentage of Corroded Area (%)	Maximum Pit Depth (mm)
1	RBA-NS-0.45-340	9.4	54.4	2.0
2	RBA-NS-0.45-400	8.7	50.3	1.5
3	RBA-NS-0.55-340	9.8	56.7	2.0
4	RBA-NS-0.55-400	9.25	53.5	2.0
5	SA-NS-0.45-340	6.5	37.6	1.0
6	SA-NS-0.45-400	5.4	31.3	No pit observed
7	SA-NS-0.55-340	5.9	34.1	1.0
8	SA-NS-0.55-400	5.55	32.1	No pit observed
9	BA-NS-0.45-340	6.6	38.2	1.0
10	BA-NS-0.45-400	6.2	35.9	No pit observed
11	BA-NS-0.55-340	6.85	39.6	1.5
12	BA-NS-0.55-400	6.4	37.0	1.0
13	RBA-RBFA-0.45-340	10.5	60.8	2.0
14	RBA-RBFA-0.45-400	9.9	57.3	1.5
15	RBA-RBFA-0.55-340-E	1.25	7.2	No pit observed
16	SA-NS-0.55-400-E	1.3	7.5	No pit observed

Table 4.5. Corroded Area and Pit Depth at Un-cracked Region

Case	Short Description	Corroded Area (cm^2)	Percentage of Corroded Area (%)	Maximum Pit Depth (mm)
1	RBA-NS-0.45-340	0.95	2.3	0.5
2	RBA-NS-0.45-400	1.12	2.7	0.5
3	RBA-NS-0.55-340	0.65	1.6	No pit observed
4	RBA-NS-0.55-400	0.8	2.0	No pit observed
5	SA-NS-0.45-340	0.0	0.0	No pit observed
6	SA-NS-0.45-400	0.15	0.4	1.0
7	SA-NS-0.55-340	0.0	0.0	No pit observed
8	SA-NS-0.55-400	0.25	0.6	No pit observed
9	BA-NS-0.45-340	0.2	0.5	No pit observed
10	BA-NS-0.45-400	0.5	1.2	No pit observed
11	BA-NS-0.55-340	0.0	0.0	No pit observed
12	BA-NS-0.55-400	0.0	0.0	No pit observed
13	RBA-RBFA-0.45-340	1.35	3.3	1.0
14	RBA-RBFA-0.45-400	0.15	0.4	0.5
15	RBA-RBFA-0.55-340-E	0.0	0.0	No pit observed
16	SA-NS-0.55-400-E	0.0	0.0	No pit observed

Higher pit depths were also observed for the cases made with RBA and BA. Based on the corroded area and corrosion pits; the corrosion activity of steel bars with the variation of aggregate can be ordered as RBA>BA>SA. Physical observation data well matched with data related to chloride ingress, macro-cell corrosion over steel bars, and

concrete resistance. Visual observation for the segmented bars at cracked region for all cases are shown on Fig. 4.14.

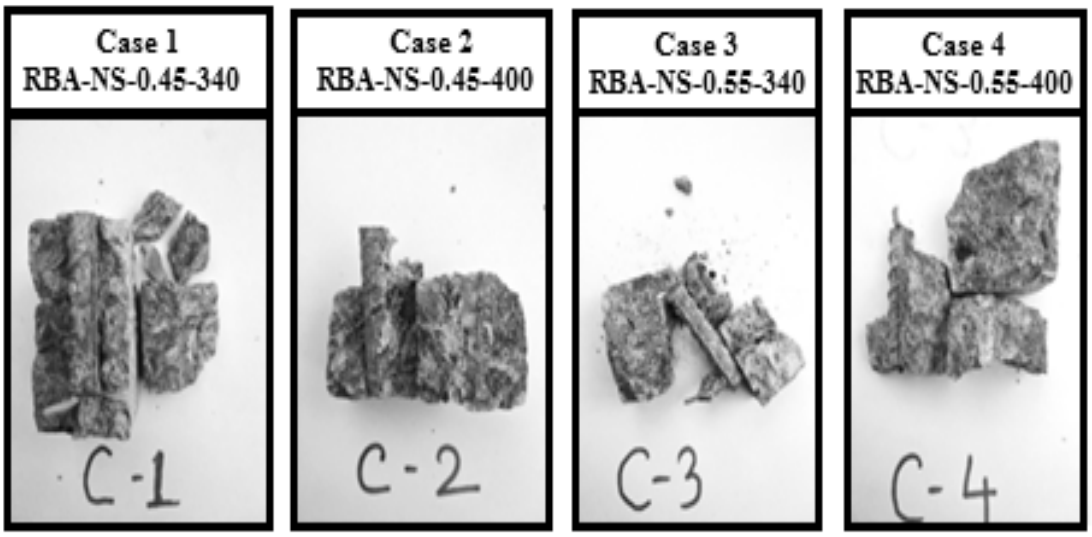

a) Concrete made with RBA as Coarse Aggregate

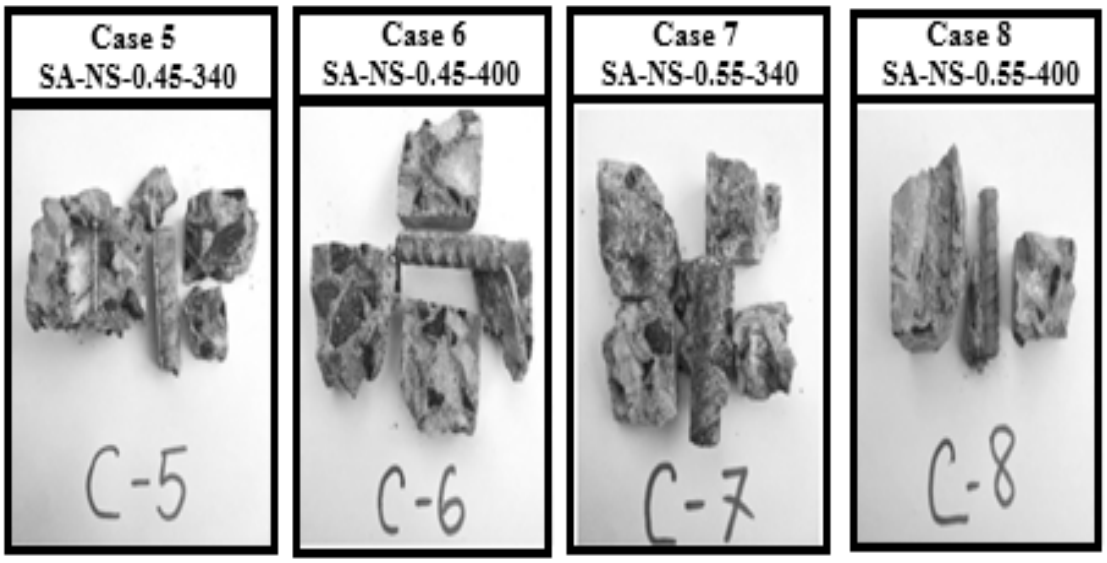

b) Concrete made with SA as Coarse Aggregate

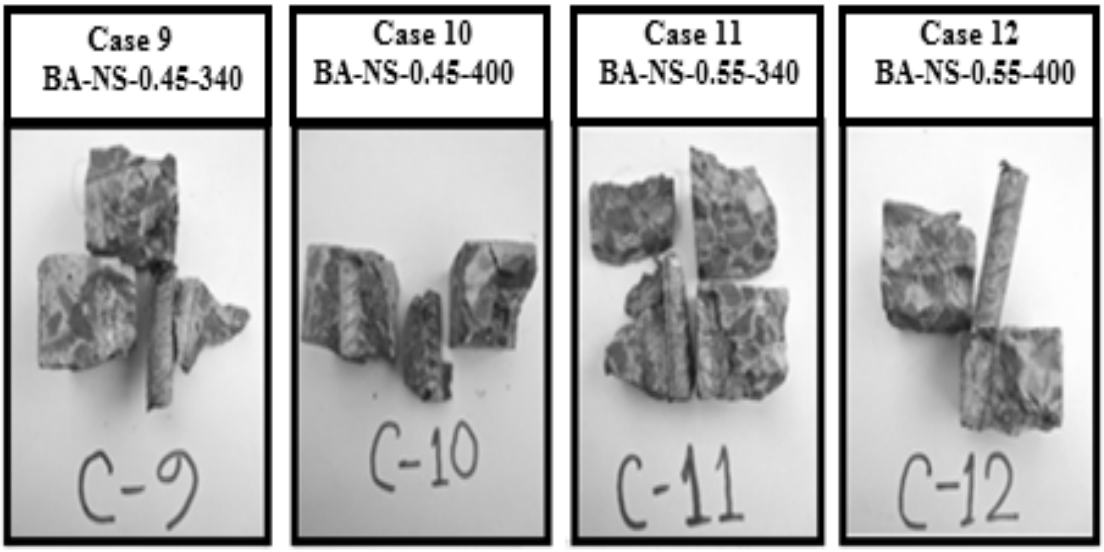

c) Concrete made with BA as Coarse Aggregate

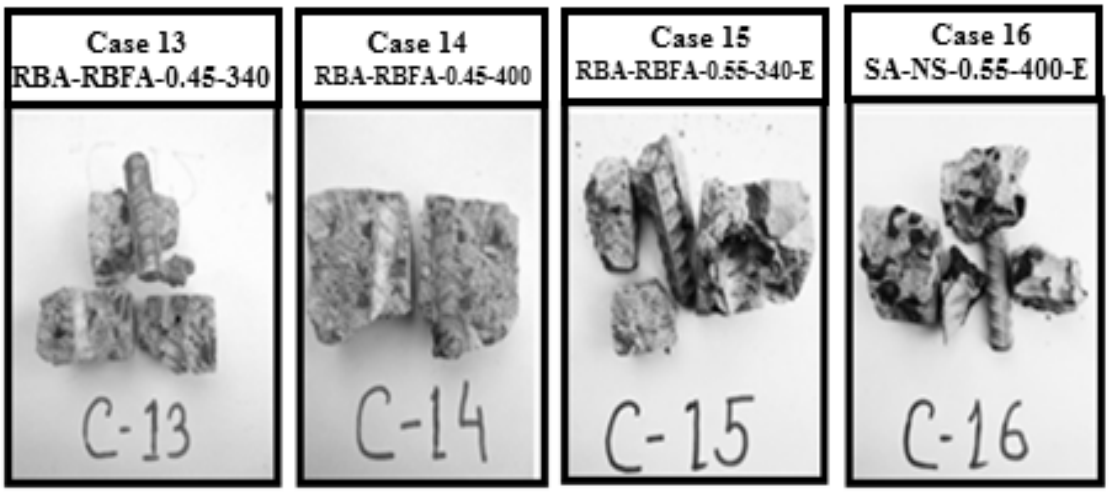

d) Concrete made with RBA as Coarse Aggregate, RBFA as Fine Aggregate, Epoxy Coated bar as Reinforcement

Fig. 4.14. Visual Observation for the Segmented bars at Cracked Region for all Cases

CHAPTER 5: CONCLUSIONS AND RECOMMENDATIONS

5.1 General

This chapter includes the summary of the research findings based on discussions in Chapter 4. Moreover, recommendations and future works related to this investigation are also proposed in this chapter.

5.2 Conclusions

Based on the experimental results of this study, the following conclusions have been drawn:

1. Chloride ingress rate in concrete with respect to types of coarse aggregate is ordered as RBA>BA>SA.

2. Macro-cell corrosion propagation with respect to types of coarse aggregate is ordered as RBA>BA>SA.

3. Epoxy coated bars exhibit least macro-cell corrosion compared to the bared steel irrespective to type of aggregates.

4. The macro-cell corrosion current density is reduced with the age of exposure period irrespective of the types of aggregates.

5. Chloride ingress as well as macro-cell corrosion current density is reduced with the reduction of w/c and with the increase of cement content in concrete.

5.3 Recommendations

From this study, it is evident that RBA and BA have shown higher rate of corrosion formation as well as chloride ingress. On the contrary stone aggregate has shown highest resistivity against chloride ingress as well as chloride induced corrosion. Hence, it can be recommended that for making construction at the marine exposures such as cyclone shelters, ports, school-colleges and for all other disaster shelters SA as coarse aggregate should be used other than RBA or BA. To use RBA and BA instead of SA, lower W/C ratio with higher cement content at the mixture design of concrete must need to be ensured.

Based on the drawn-out summaries, following recommendations for future work can be made:

a) Further works can be planned to monitor the long term effects due to both micro-cell and macro-cell corrosion and corresponding chloride ingress amounts.

b) The scope of the research can be expanded by using other types of cements such as CEM Type II BM, CEM Type II BMSL, various compositions of OPC and Slag cements such as 15% OPC with 85% slag content, 30% OPC with 70% slag, 80% OPC and 20% etc. to study the effect of different types of cements on chloride ingress and chloride induced corrosion rates.

c) The effects of variation of humidity on corrosion of steel bars inside concrete can be monitored by maintaining different amount of humidity at the specialized salt spray chamber.

d) The effects of variation of temperature on corrosion of steel bars inside concrete can be monitored by maintaining different amount of temperature at the specialized salt spray chamber.

e) The scope of the research can be expanded by adding more values of W/C ratios and cement content amounts in the mix designs.

f) Various coated aggregate can be used in future research work and the difference of corrosion and chloride ingress rate can be analyzed for designing more durable structure at marine exposure.

g) Different chemical additives can be applied to reduce the overall corrosion rate and chloride ingress, so that RBA and BA can be used as alternative to SA in the construction work ensuring safety and durability.

REFERENCES

Alexander, K.M., and Ivanusec I. (1982), “Long term effects of cement SO_3 content on the properties of normal and high-strength concrete, Part I. The effect on strength”, *Cement and Concrete Research*, Vol. 12, No. 1, pp. 51–60.

Ali, S.P., Dehghanian, C., and Kosari, A. (2015), “Corrosion protection of the reinforcing steels in chloride-laden concrete environment through epoxy/polyaniline–camphor sulfonate nanocomposite coating”, *Corrosion Science*, 90, 239-247.

Alonso, C., Andrade, C., Novoa, X. R., Izquierdo, D., and Perez, M. C. (1998), "Effect of protective oxide scales in the macro galvanic behavior of concrete reinforcements", *Corrosion Science*, 40(8), 1379-1389.

American Concrete Institute (1996), “Corrosion of metals in concrete”, *ACI Committee*, ACI 222-96.

Ann, K.Y. and Song, H. W. (2007), "Chloride threshold level for corrosion of steel in concrete", *Corrosion Science*, 49(11), 4113.

Andrade, C., and Alonso, C. (2004), "Test methods for on-site corrosion rate measurement of steel reinforcement in concrete by means of polarization resistance method", *Materials and Structures*, 37(9), 623-643.

Andrade. C., and Alanso, C. (2001), “On-site measurements of corrosion rate of reinforcements”, *Construction and Building Materials*, 15, 141-145.

Andrade, C., Soler, L., and Novoa, X. R. (1995), "Advances in electrochemical impedance measurements in reinforced concrete", *Materials Science Forum*, 192-194, 843-56.

Andrade, C.M., Feliu, S., Feliu, J.A., and Feliu, J.S. (1992), “The effects of macrocells between active and passive areas of steel reinforcements”, *Corrosion Science*, Vol: 33(2), page: 237-249.

Andrade, C., and Gonzales, J. A. (1978), "Quantitative measurements of corrosion rate of reinforcing steels embedded in concrete using polarization resistance measurements", Materials and Corrosion, 29, 515-519.

Arya, C., and Ofori, F.K. (1996), “Influence of crack frequency on reinforcement corrosion in concrete”, Cement and Concrete Research, 26(3), 345-353.

Arup, H. (1983), "The mechanisms of the protection of steel by concrete", Society of Chemical Industry Conference of Reinforcement in Concrete Construction London, 151.

Arya, C., and Newman J.B. (1990), "Problem of predicting risk of corrosion of steel in chloride contaminated concrete", ICE Proceedings, 88, 875.

ASTM C 192, (2003), "Standard test method for making and curing concrete test specimens in the laboratory", *American Society for Testing and Materials.*

ASTM C39/C39M-16 (2016), “Standard test method for compressive strength of cylindrical concrete specimens”, *ASTM International*, West Conshohocken, PA.

ASTM C 39 (2003), "Standard test method for compressive strength of cylindrical concrete specimen", *American Society for Testing and Materials.*

Balma, J., Darwin, D., Browning, J. P., and Locke, C. E. (2005), "Evaluation of corrosion protection systems and corrosion testing methods for reinforcing steel in concrete", SM Report No. 76, The University of Kansas Center for Research, Inc., Lawrence, KS.

Baweja, D., Roper, H., and Sirivivatnanon, V. (2003), "Improved electrochemical determinations of chloride induced steel corrosion in concrete", *ACI Materials Journal*, 100(3), 228-238.

Barneyback., R.S. and Diamond, S. (1981), "Expression and analysis of pore fluids from hardened cement pastes and mortars", *Cement and Concrete Research*, 11(2), 279.

Beshr, H., Almusallam, A. A., and Maslehuddin, M. (2003), "Effect of coarse aggregate quality on the mechanical properties of high strength concrete", *Construction and Building Materials*, Vol.17, No.2, pp.97-103.

Berke, N. S., Aldykiewicz, A. J., and Lianfang, L. (2003), "What's new in corrosion inhibitors? ", Structure, NCSEA, CASE, SEI, 10-12.

Bentur, A. (1997), "Steel corrosion in concrete: Fundamentals and civil engineering practice", E & FN Spon, London.

Broomfield, J. P. (1997), "Corrosion of steel in concrete: Understanding, investigation, and repair", E & FN Spon, London.

Berkely, K. G. C., and Pathmanaban, S. (1990), "Cathodic protection of reinforcement steel in concrete", Butterworths - Heinemann, London.

Castellote, M., Alonso, C., Andrade, C., Castro, P., and Echeverria, M. (2001), "Alkaline leaching method for the determination of the chloride content in the aqueous phase of hardened cementitious materials", *Cement and Concrete Research*, 31(2), 233.

Castellote, M., Andrade, C., and Alonso, C. (2002), "Accelerated simultaneous determination of the chloride depassivation threshold and of the non-stationary diffusion coefficient values", *Corrosion Science*, 44(11), 2409-2424.

Cella, P. A., and Taylor, S. R. (2000), "Electrical resistance changes as an alternate method for monitoring the corrosion of steel in concrete and mortar", *Corrosion*, 56(9), 951-959.

Chang, Z.-T., Cherry, B., and Marosszeky, M. (2007), "Polarization behavior of steel bar samples in concrete in seawater part 1: Experimental measurement of polarization curves of steel in concrete", *Corrosion Science*, In Press, Corrected Proof.

Chappelow, C. C., McElroy, A. D., Blackburn, R. R., Darwin, D., Noyelles, F. G. D., and Locke, C. E. (1992), "Handbook of test methods for evaluating chemical deicers", SHRP-

H-332, Strategic Highway Research Program, National Research Council, Washington, DC.

Clear, K. C. (1992). "Effectiveness of epoxy-coated reinforcing steel", *Concrete International*, 14(5), 58-64.

Cody, R. D., Cody, A. M., Spry, P. G., and Gan, G. (1996), "Experimental deterioration of highway concrete by chloride deicing salts", Environmental & Engineering Geoscience, II(4), 575-588.

CRSI. (1995), "Adhesion loss mechanisms of epoxy coatings on rebar surfaces", Surface Science Western, Concrete Reinforcement Steel Institute, Schaumburg, IL.

Darwin, D., Browning, J. P., Ngyuen, T. V., and Locke, C. E. (2002), "Mechanical and corrosion properties of a high-strength, high chromium reinforcing steel for concrete", SD2001-05-F, University of Kansas Center for Research, Inc., Lawrence, Kansas.

Demirboga, R., and Gul, R. (2006), "Production of high strength concrete by use of industrial by-products", *Building and Environment*, Vol.41, No.8, pp.1124-1127.

Dhir, R. K., McCarthy, M.J., Zhou, S., and Tittle, P. A. J. (2004), "Role of cement content in specifications for concrete durability: Cement type influences", *Structures and Buildings*, No. 157, *Institution of Civil Engineers,* U.K., Vol.157, No.2, pp.113-127.

Elsener, B., and Bohni, H, (1992), "Electrochemical methods for the inspection of reinforcement corrosion in concrete structures - field experience", *Materials Science Forum*, 111-112, 635-647.

Feliu, S., Gonzalez, J. A., Andrade, M. C., and Feliu, V. (1988), "Determination of polarization resistance in reinforced concrete slabs", *Corrosion*, 44(10), 761-765.

Feliu, S., Gonzalez, J. A., Escudero, M. L., Feliu Jr., S., and Andrade, M. C. (1990). "Possibilities of the guard ring for electrical signal confinement in the polarization measurements of reinforcements", *Corrosion*, 46(12), 1015-1020.

Feng, Z.S., Chun-hua, L., and Rong-gui, L. (2011), "Experimental determination of chloride penetration in cracked concrete of beams", International Conference on Advances in Engineering, Procedia Engineering 24, page: 380-384.

Gaal, G.C.M. (2004), "Prediction of deterioration of concrete bridges corrosion of reinforcement due to chloride ingress and carbonation", PhD thesis, Technical University at Delft, Delft, Netherland.

Gaag, C.R., (2014), "Cement and concrete as an engineering material: An historic appraisal and case study analysis", *Engineering Failure Analysis,* Volume 40, Pages 114-140.

Glass, G. K., and Buenfeld, N. R. (1997), "The presentation of the chloride threshold level for corrosion of steel in concrete", *Corrosion Science*, 39(5), 1001-1013.

Hansson, C.M., Poursaee, A., and Laurent, A. (2006), "Macrocell and microcell corrosion of steel in ordinary Portland cement and high performance concretes", *Cement and concrete research*, vol: 36, page: 2098-2102.

Hassoun, M. N., and Al-Manaseer, A. (2008), "Structural concrete: Theory and design", 4th Edition., Canada: John Wiley and Sons, Inc.

Hope, B.B., and Alan K.C. (1987), "Corrosion of steel in concrete made with slag cement", Technical paper, *ACI Materials Journal*, Title No: 84-M47.

Hope, B. B., Page, J. A., and Poland, J. S. (1985), "The determination of the chloride content of concrete", *Cement and Concrete Research*, 15(5), 863.

Hossain, M. (2012), "Securing the environment: Potentiality of green brick in Bangladesh", *BUP Journal,* Vol.1, No.1, pp.79–89.

Kahrs, J. T., Darwin, D., and Locke, C. E. (2001), "Evaluation of corrosion resistance of type 304 stainless steel clad reinforcing bars", University of Kansas Center for Research, Inc., Lawrence, Kan.

Kakizaki, M., Edahiro, H., Tochigi, T., and Niki, T. (1992), “Effect of mixing method on mechanical properties and pore structure of ultra-high-strength concrete”, *ACI Special Publication*, Vol. 132, pp. 997–1016.

Kobayashi, K., Takewaka, K. (1984), “Experimental studies on epoxy coated reinforcing steel for corrosion protection”, *International Journal of Cement Composites and Lightweight Concrete*. 6(2) (1984) 99-116.

Kropp, J. (1995), “Relations between transport characteristics and durability”, Rilem Report 12- Performance criteria for concrete durability. State of the art report by Rilem TC 116-PCD. E & FN Spon, p. 65–89.

Lamond, J. F., and Pielert, J. H. (2006), "Significance, tests and properties of concrete and concrete-making materials", *ASTM International*, Vol.10, No. 41, pp. 65–67.

Layssi, H., Ghods, P., Alizadeh, A.R., and Salehi, M. (2015), “Electrical resistivity of concrete”, *Concrete International*. pp. 41–46.

Liu, Y., and Weyers, R. E. (2003), "Comparison of guarded and unguarded linear polarization CCD devices with weight loss measurements", Cement and Concrete Research, 33(7), 1093-1101.

Lopez, H.Z., Kandratova, I., Bremner, T.W., and Thomas, M.D.A. (2012), “Epoxy-coated bars as corrosion control in cracked reinforced concrete”, *Materials and Corrosion*. 64(7), 599-608.

Li, Z. (2011), “Advanced concrete technology: John Wiley and Sons”, ISBN 9780470902431.

Hossain, M., and Abdullah, A.M. (2012), “Securing the environment: Potentiality of green brick in Bangladesh”, *BUP Journal*, Volume 1, Issue 1, ISSN: 2219-4851.

Jovancicevic, V., Bockris, J. O. M., Carbajal, J. L., Zelenay, P., and Mizuno, T. (1986), "Adsorption and absorption of chloride ions on passive iron systems", *Journal of the Electrochemical Society*, 133(11), 2219-2226.

Martinez, S. L., Darwin, D., McCabe, S. L., and Locke, C. E. (1990), "Rapid test for corrosion effects of deicing chemicals in reinforced concrete", SL Report 90-4, University of Kansas Center for Research, Lawrence, KS.

Ma, Z.,Duan, Z., and B. (2019), “Effects of an applied load on the chloride penetration of concrete with recycled aggregates and recycled powder”, *Advances in Civil Engineering*, Volume 2019, Article ID 1340803, 15 pages.

Maslehuddin, M., Sharif, M. A., Shameem, M., Ibrahim, M., and Barry, M. S. (2003), "Comparison of properties of steel slag and crushed limestone aggregates", *Constr. Build. Material.,* Vol.17, No.2, pp.105–112.

McDonald, D. B., Pfeifer, D. W., and Sherman, M. R. (1998), "Corrosion evaluation of epoxy-coated, metallic clad, and solid metallic reinforcing bars in concrete", FHWA-RD-98-153, Federal Highway Administration, McLean, VA.

Medgar, L. M., Nisbet, M. A., and Van Geem, M. G. (2006), "Life cycle inventory of Portland cement manufacture", *PCA Rand Serial No. 2095b. Skokie*, IL: Portland Cement Association.

Mehta, K. P., and Monteiro, P. J. M. (1993), "Concrete structure, properties, and materials", 2nd Edition, Prentice Hall, New Jersey.

Mindess, S., Young, J. F., and Darwin, D. (2003), "Concrete", 2nd Ed., Prentice-Hall Inc., Englewood Cliffs, New Jersey.

Miyaji, M., Okazaki, K., and Ochaii, C. (2017), "A study on the use of cyclone shelters in Bangladesh", 82 (737), 1871-1880, July 2017.

Mohammed, T.U., Otsuki, N., Hisada, M., and Tsunenori, S. (2001), "Effect of crack width and bar types on corrosion of steel in concrete", *Journal of Materials in Civil Engineering*, 13 (3), 194-201.

Mohammed, T. U., Hidenori, H., and Toru, Y. (2001), "Macro-cell and micro-cell corrosions of steel bars in cracked concrete exposed to marine environment", 5th CANMET/ ACI International Conference on recent advances in concrete technology, Singapore, Vol: Supplementary volume, pp. 155- 169.

Mohammed, T.U., Hamada, H., and Yokota, H. (2004), "Macro-cell and micro-cell corrosion of steel bars in cracked concrete made with various cements", *ACI Materials Journal*, Vol: 221, page: 51-72.

Mohammed, T.U., Otsuki, N., and Hamada, H. (2003), "Corrosion of steel bars in cracked concrete under marine environment", *Materials in Civil Engineering*, 15, No.5.

Mohammad, T.U., Otsuki, N., and Hamada, H. (2003), "Corrosion of steel bars in cracked concrete under marine environment", ASCE, *Journal of Material in Civil Engineering*, 15,460-469,DOI: 10.1061/(ASCE)0899-1561(2003)15:5(460).

Mohammed, T.U., Otsuki, N., and Hamada, H. (2003), "Corrosion of steel bars in cracked concrete under marine environment", *Journal of Materials in Civil Engineering*, Vol.15, No.5.

Mohammed, T. U., Hasnat, A., Sarwar, N., Das, H. K., Miah, J. M., and Awal, M. A. (2011), "Sustainable development of construction works in Bangladesh", The 3rd International Conference of EACEF (European Asian Civil Engineering Forum), pp. 271–277.

Mohammed, T.U., Otsuki N., Hamada, H., and Yamaji, T. (2011), "Macro-cell and micro-cell corrosions of steel bars in cracked concrete exposed to marine environment", 5th CANMET/ACI International Conference on recent advances in concrete technology, Singapore, Supplementary volume, pp. 155- 169.

Mohammed, T.U., Hamada, H., Mamun, M.A.A., and Hasnat, A. (2013), "Corrosion of cement paste coated steel bars in marine environment" 3rd International Conference on Sustainable Construction Materials and Technologies (SCMT3).

Mohammed, T.U., Ariful, H., Mohammad, A.A., and Shamim, Z.B. (2013), "Recycling of brick aggregate concrete: an extended study on some key issues", Third International Conference on Sustainable Construction Materials and Technologies (SCMT3).

Mohammed, T.U., Hamada, H.,Mamun, M.A.A., and Hasnat, A. (2013), "Corrosion of cement paste coated steel bars in marine environment", 3rd International Conference on Sustainable Construction Materials and Technologies (SCMT3), Japan.

Mohammed, T. U., Hasnat, A., Awal, M. A., and Bosunia, S. Z. (2014), "Recycling of brick aggregate concrete as coarse aggregate", *ASCE Journal of Materials in Civil Engineering*, Vol. 27, pp. 1–9.

Mohammed, T.U., Khan, A. Z., and Mahmood, A.H. (2015), "Recycling of demolished brick aggregate concrete as coarse and fine aggregates", International Conference on the Regeneration and Conservation of Concrete Structures (RCCS), Nagasaki, Japan, pp. 1-12.

Mohammed, T.U., Khan, A.Z., and Mahmood, A.H. (2015), "Recycling of demolished brick aggregate concrete as coarse and fine aggregates", International Conference on the Regeneration and Conservation of Concrete Structures (RCCS), Nagasaki, Japan, pp. 1-12.

Mohammed, T.U., Masud, M.M.U., Rahman, M., and Mamun, M.A.A. (2019), "Effects of cement types on chloride ingress in concrete", The 3rd ACF Symposium, Hokkaido University, Japan.

Nanayakakkara, O., and Kato, M. (2009), “Macro-cell corrosion in reinforcement of concrete under non-homogeneous chloride environment”, *Journal on Advanced Concrete Technology*. 7(1), 31-40.

Nygaard, P., and Geiker, M. (2005), "A method for measuring the chloride threshold level required to initiate reinforcement corrosion in concrete", *Materials and Structures*, 38(4), 489-494.

Page, C. L., and Vennesland, Q. (1983), "Pore solution composition and chloride binding capacity of silica-fume cement pastes", Materiaux Et Constructions, 16(91), 19.

Popovics, S. (1990), "Analysis of the concrete strength versus water-cement ratio relationship", *ACI Materials Journal*, Vol.87, No.5, pp.517–529.

Price, W., Jones, M., Ting, S., and Dhir, R. (2003) “Effect of aggregate porosity on chloride ingress into concrete”, Proceedings of the International Symposium dedicated to Professor Surendra Shah, Northwestern University, USA held on 3–4 September 2003 at the University of Dundee, Scotland, UK.

Pyc, W., Weyers, R. E., Sprinkel, M. M., Weyers, R. M., Mokarem, D. W., and Dillard, J. G. (2000), "Performance of epoxy-coated reinforcing steel", *Concrete International*, 22(2), 57-62.

Ramezanianpour, A.A., Ghoreishian, S.A.H., Ahmadi, B., Balapour, M., and Ramzezanianpour, A.M., (2018), “Modelling of chloride ions penetration in cracked concrete structures exposed to marine environment”, International Federation for Structural Concrete, 1-12.

Relim (1988), “Corrosion of steel in concrete. State of the art report”, Committee 60-CSC, Chapman & Hall, London.

Rixom, R., and Mailvaganam, N. (1999), "Chemical admixtures for concrete", 3rd Ed., Taylor and Francis, E and FN Spon.

Rodríquez, P., Ramirez, E., and Bonzales, J. A. (1994), "Method for studying corrosion in reinforced concrete", Concrete Research Magazine, 46(167), 81-90.

Sarker, D. (2015), "Reduction of carbon emission by using green bricks: Bangladesh perspective", *International Journal of Engineering Trends and Technology*, Vol.24, No.1, pp.15–20.

Sagues, A. A., Powers, R. G., and Kessler, R. (1994), "Corrosion processes and field performance of epoxy-coated reinforcing steel in marine structures", *Corrosion* 94, National Association of Corrosion Engineers (NACE), Houston, TX, Paper number 229.

Sehgal, A., Kho, Y. T., Osseo-Asare, K., and Pickering, H. W. (1992), "Reproducibility of polarization resistance measurements in steel-in-concrete systems", *Corrosion*, 48, 706-714.

Sofia, R., and Bogas, J.A., (2018), "Chloride ingress into structural lightweight aggregate concrete in real marine environment", *Marine Structures*, 61, 170–187.

Schulze, J. (1999), "Influence of water-cement ratio and cement content on the properties of polymer-modified mortars", *Cement and Concrete Research*, Vol.29, No.6, pp.909–915.

Sizov, V. P. (1997), "Effect of sand content in concrete and aggregate size on cement consumption and strength of concrete", *Hydrotechnical Construction*, Vol.31, No.3, pp. 194–196.

Schwensen, S. M., Darwin, D., and Locke, C. E. (1995), "Rapid evaluation of corrosion resistant concrete reinforcing steel in the presence of deicers", SL Report 95-6, University of Kansas Center for Research, Inc., Lawrence, KS.

Senecal, M. R., Darwin, D., and Locke, C. E. (1995), "Evaluation of corrosion-resistant steel reinforcing bars", SM Report No. 40, University of Kansas Center for Research, Inc., Lawrence, KS.

Song, H.-W., and Saraswathy, V. (2007), "Corrosion monitoring of reinforced concrete structures - a review", *International Journal of Electrochemical Science*, 2, 1-28.

Soleymani, H. R., and Ismail, M. E. (2004), "Comparing corrosion measurement methods to assess the corrosion activity of laboratory OPC and HPC concrete specimens", *Cement and Concrete Research*, 34(11), 2037.

Stern, M., and Geary, A. L. (1957), "A theoretical analysis of the shape of polarization curves", *Journal of the Electrochemical Society*, 104, 56.

Smith, J. L., Darwin, D., and Locke, C. E. (1995), "Corrosion-resistant steel reinforcing bars", SL Report 95-1, University of Kansas Center for Research, Inc., Lawrence, KS.

Smith, J. L., and Virmani, Y. P. (1996), "Performance of epoxy-coated rebars in bridge decks", FHWA-RD-96-092, Federal Highway Administration, McLean, VA.

Su, J. K., Cho, S. W., Yang, C. C., and Huang, R. (2002), "Effect of sand ratio on the elastic modulus of self-compacting concrete", *Journal of Marine Science and Technology*, Vol.10, No.1, pp.8–13.

Tuutti, K. (1982), “Corrosion of steel in concrete”, Swedish Cement and Concrete Research Institute, Stochkolm.

Videm, K. (2001), "Phenomena disturbing electrochemical corrosion rate measurements for steel in alkaline environments", *Electrochimica Acta*, 46(24-25), 3895-3903.

Viedma, P. G., Castellote, M., and Andrade, C. (2006), "Comparison between several methods for determining the depassivation threshold value for corrosion onset" *Journal of Physique IV*, 136, 79-88.

Wassermann, R., Katz, A., and Bentur, A. (2009), "Minimum cement content requirements: a must or a myth", *Materials and Structures*, Vol.42, No.7, pp.973–982.

Weyers, R. E., Sprinkel, M. M., Pyc, W., Zemajtis, J., Liu, Y., and Mokarem, D. W. (1998), "Field investigation of the corrosion protection performance of bridge decks and piles constructied with epoxy-coated reinforcing steel in virginia", VTRC 98-R4, Virginia Transportation Research Council, Charlottesville, VA.

Wipf, T. J., Phares, B. M., and Fanous, F. S. (2006), "Evaluation of corrosion resistance of different steel reinforcement types", CTRE Project 02-103, Center for Transportation Research and Education, Iowa State University, Ames, IA.